



# Chemical syntheses of bioinspired and biomimetic polymers toward biobased materials

Mitra S. Ganewatta<sup>1</sup>, Zhongkai Wang<sup>2</sup> and Chuanbing Tang<sup>1</sup>

**Abstract** | The rich structures and hierarchical organizations in nature provide many sources of inspiration for advanced material designs. We wish to recapitulate properties such as high mechanical strength, colour-changing ability, autonomous healing and antimicrobial efficacy in next-generation synthetic materials. Common in nature are non-covalent interactions such as hydrogen bonding, ionic interactions and hydrophobic effects, which are all useful motifs in tailor-made materials. Among these are biobased components, which are ubiquitously conceptualized in the space of recently developed bioinspired and biomimetic materials. In this regard, sustainable organic polymer chemistry enables us to tune the properties and functions of such materials that are essential for daily life. In this Review, we discuss recent progress in bioinspired and biomimetic polymers and provide insights into biobased materials through the evolution of chemical approaches, including networking/crosslinking, dynamic interactions and self-assembly. We focus on advances in biobased materials; namely polymeric mimics of resilin and spider silk, mechanically and optically adaptive materials, self-healing elastomers and hydrogels, and antimicrobial polymers.

Living matter has long been a source of inspiration for conceiving new chemistry and functional structures, materials and devices<sup>1–4</sup>. Nature performs with high precision on every level, from molecules to aggregates to whole organisms. For example, spider silk<sup>5,6</sup>, insect resilin<sup>7,8</sup> and sea cucumber dermis<sup>9</sup> have desirable tensile strength, resilience and dynamic stiffness, respectively, and we would like to have synthetic functional materials with the same properties. Natural selection, rather broadly, facilitates the survival of species with beneficial traits. Hence, biological designs actively change in response to biophysical stimuli, exhibiting adaptive growth, self-assembly and self-repair<sup>10,11</sup>. Researchers have attempted to elucidate the fundamental molecular features of biological objects and discover the underlying principles responsible for their unique properties, which have experienced substantial refinements over millions of years<sup>12,13</sup>. These features are relevant to various length scales — single molecule, surface or bulk — and manifest themselves as antimicrobial activity<sup>14</sup>, superhydrophobicity/superhydrophilicity<sup>15,16</sup>, drag reduction<sup>17</sup>, wet adhesion<sup>18</sup>, mechanical strength<sup>19</sup>, structural colouration<sup>20</sup>, thermal management<sup>21</sup> and self-healing<sup>22,23</sup>, to name a few. Gaining knowledge of these features is essential to develop sophisticated materials to solve environmental, social and economic challenges ranging from climate change<sup>24</sup> to resource security<sup>25</sup> and public health<sup>26</sup>. New technologies, including advanced

microscopic/nanoscopy characterization tools, computational methods and precision syntheses, have led to remarkable progress in understanding and mimicking biological functions and properties, thereby offering new opportunities in biomimetic and bioinspired materials<sup>27,28</sup>.

At this point, it is beneficial to clarify the distinction between the terms ‘bioinspired’ and ‘biomimetic’. Standard definitions, including industry standards such as VDI 6220 and ISO 18458, were established recently<sup>11,29,30</sup>. These sources describe biomimetics/biomimicry as a field of research in which one recreates or imitates the structures and/or functions of complicated biological systems in non-living systems using simplified or adapted mechanisms. Fabricating peptides to mimic natural antimicrobial peptides (AMPs) is a classic example. In contrast, bioinspiration is the development of novel materials, devices and structures with advantageous properties and in increasingly complex ways. The development is based on lessons from biological systems, in regard to physical and chemical properties, structures and functions. For example, AMP-inspired cationic acrylate polymers that perform antimicrobial functions are solely bioinspired. Therefore, bioinspiration is more encompassing and differs from biomimicry in that the latter aims to precisely imitate the biological system. Synthetic mimics of natural systems require extensive research to achieve a level of sophistication and function

<sup>1</sup>Department of Chemistry and Biochemistry, University of South Carolina, Columbia, SC, USA.

<sup>2</sup>Biomass Molecular Engineering Center, Anhui Agricultural University, Hefei, China.

✉e-mail:  
tang4@mailbox.sc.edu  
<https://doi.org/10.1038/s41570-021-00325-x>

on par with biological systems. The field of biomimetic polymers focuses on exploring molecular building blocks (for example, end groups and repeating units), macromolecular assembly (for example, polymer–polymer interactions), hierarchical organization and mesoscale and macroscale phenomena that result in mechanical strength, self-healing and structural colours.

Increasing attention has been paid to the translation of biological concepts into applications for sustainable development. Polymers derived from renewable resources are emerging as full or partial replacements for petrochemical-based materials, including elastomers, plastics, hydrogels, resins and composites<sup>31–33</sup>. The adoption of renewable biobased feedstocks is vital for reducing the global carbon footprint of plastics<sup>34</sup> and creating sustainable polymers that are environmentally innocuous<sup>35</sup>. Beyond renewability, biobased materials could bring new functionalities leading to better performance, biocompatibility and biodegradability<sup>36</sup>. Renewable feedstocks are available as biopolymers such as cellulose, lignin, chitin or polyhydroxyalkanoates. Alternatively, one can renewably source molecular building blocks, including lactic acid, terpenes, fatty acids and carbon dioxide, providing opportunities to design a variety of biobased biomimetic and bioinspired materials by biopolymer modification or monomer engineering<sup>31,37,38</sup>. In this Review, we describe how recent advances in bioinspired and biomimetic polymer research help us develop chemical approaches to sustainable biobased materials (FIG. 1). Although these are vast research areas, we focus on biobased polymers that can recapitulate the most representative properties in the bulk or at the macromolecular level. Among bulk biobased materials, mechanical properties are widely conceived to be

crucial for versatile functions and applications. Thus, we have chosen to discuss resilin and spider silk mimics, mechanically adaptive materials and self-healing materials, which exemplify a broad spectrum of bulk mechanical behaviour ranging from soft to strong and to stimuli responsive. Moving from bulk to macromolecular properties, we consider antimicrobial efficacy as an example of a useful trait on this scale. Examples of systems that rely on both bulk and macromolecular properties include optically adaptive materials, and we describe these as a case study in how great precision at the molecular level must be complemented by appropriate macroscopic properties to satisfy application demands. To highlight each biomimetic and bioinspired material, we detail molecular-level features (in particular, antimicrobial activity) and macroscopic properties such as mechanical strength and structural colours.

### Polymer mimics with outstanding mechanical properties

Biomimetic and bioinspired structures have their origins in unique naturally occurring systems<sup>39,40</sup>. Indeed, materials such as nacre (mother-of-pearl), muscle, resilin and spider silk have fascinating mechanical properties, with nacre in particular exhibiting extraordinary strength and toughness, due to the brick-and-mortar microstructures<sup>41,42</sup>. The large protein titin undergoes reversible folding to endow muscle tissue with remarkable toughness, strength and elasticity<sup>43,44</sup>. Similarly, resilin proteins combine high resilience, high strain, low stiffness and prolonged fatigue lifetime<sup>45,46</sup>. In contrast, spider silk is among the organic materials with high mechanical strength and toughness<sup>47,48</sup>. This section covers the design and synthesis of polymeric materials

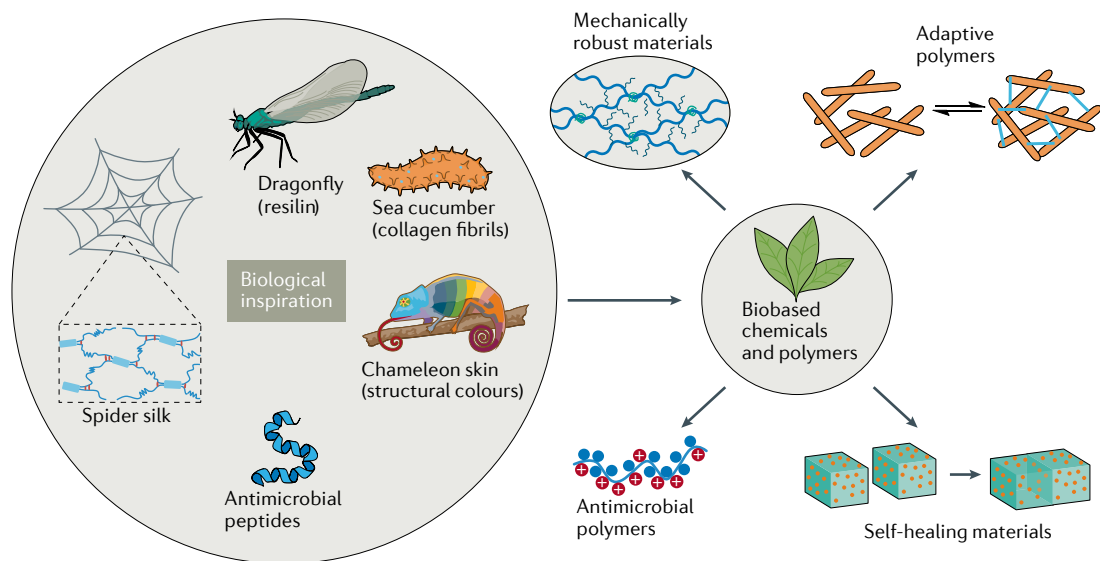


**Fig. 1 | Chemistry of bioinspired and biomimetic polymers and their biobased mimics.** Sources of inspiration can be obtained from organisms and natural biomaterials. Improved technologies enable us to better understand biomolecular function so we can develop bioinspired materials. For example, the outstanding mechanical properties of spider silk are due to the combined effects of separate crystalline and hydrogen-bonded amorphous regions of the matrix<sup>26</sup>. Biobased chemicals and polymers are increasingly available for creative material development<sup>27</sup>. The sustainable biomimetic and bioinspired materials described in this Review are categorized as mechanically robust materials (including resilin mimics and spider silk mimics), mechanically and optically adaptive polymers, self-healable materials and antimicrobial polymers.

that mimic the chemical compositions, microstructures and mechanical properties of resilin and natural silk.

**Resilin-mimicking materials.** High resilience is the ability to undergo substantial reversible deformation with negligible energy loss for elastic materials. First discovered in the elastic tendons of dragonflies in the early 1960s, resilin exhibits high resilience, large extensibility and low elastic modulus, which play a vital role in insect flight, sound production and locomotion<sup>49</sup>. Resilin has more than 95% resilience (with tensile strength greater than 1 MPa), which is probably the highest of all natural materials<sup>45</sup>. Although the resilin pads and tendons in insects can be easily isolated for characterization, the use of natural resilin as a structural material is virtually impossible due to its scarcity. To closely mimic the mechanical properties of resilin, we must consider the molecular structure–property relationships. The rubber-like elastomeric sequence in resilin is involved in the entropy-driven mechanism of elastic recoil (FIG. 2a). The polypeptide chain is highly flexible, intrinsically disordered and covalently crosslinked at a Tyr residue<sup>45,50</sup>. Well-defined chemical networks with uniform chain length, long and flexible polymeric chains, and low intermolecular friction are responsible for high resilience and minimal energy loss. We can best mimic resilin by first introducing small molecular lubricants and/or lowering chain entanglement to offer high chain flexibility and low intermolecular friction. Second, crosslinking chemistry builds diverse networks that facilitate high elasticity. Biological protein mimics made through gene expression and synthetic mimics such as hydrogels and elastomers are the two major classes of resilin-mimicking materials.

A resilin-like polypeptide (RLP) can be designed and prepared by biosynthetic gene expression<sup>51</sup>. In this way, large quantities of soluble RLPs can be produced and cast into films that serve as structural materials. For example, pentadecapeptide (GGRPSDSYGA<sub>12</sub>GGGN) and tridecapeptide (GYSGGRPGGQDLG) repeats afford amorphous and highly flexible molecular structures<sup>52</sup>. Moreover, hydrophilic sequences of RLPs are readily hydrated and exhibit low intermolecular friction. After crosslinking, the synthetic biomaterials exhibit high resilience comparable to that of natural resilin.

Besides cloning and expression techniques, the construction of chemical networks plays a crucial role in forming materials with high resilience. Dityrosine crosslinks are common motifs in biomaterial designs<sup>53</sup> and are particularly important for tuning the assembly and mechanical properties of resilin-like materials, including RLPs<sup>53</sup> (FIG. 2b). Dityrosines form during Ru<sup>II</sup>-mediated photocrosslinking of a cloned soluble protein that represents the elastic region in natural protein (rec1-resilin)<sup>54</sup>. The rapid, quantitative and controllable oxidative coupling converts the protein molecules into networks with high resilience (92%) and a large elongation at break (300%)<sup>55</sup>. It is also possible to start with recombinant exon-encoded resilins<sup>56</sup> and crosslink Tyr residues in the exons through a horse-radish peroxidase-catalysed radical reaction to yield a highly elastic biomaterial with 94% resilience. Lastly,

the crosslinking of recombinant resilin by means of a photo-Fenton reaction can also afford dityrosines<sup>56</sup> as part of highly resilient (96%) and adhesive biomaterials.

As we have noted, natural resilin is hydrophilic, and the solvation affords low intermolecular friction and high resilience. To ensure that synthetic RLPs are similarly hydrated, they can be expanded into hydrogels with diverse crosslinking routes aside from Tyr coupling. For example, Mannich-type condensation between a Lys side chain and hydroxymethylphosphine affords a new class of resilient hydrogels<sup>57</sup> (FIG. 2b), and by tuning crosslink density, one can make RLP-based hydrogels with high (90–98%) resilience. Alternatively, Cys residues on a recombinant RLP undergo Michael-type addition to a multi-arm poly(ethylene glycol) (PEG) macromer bearing vinyl sulfones to give versatile hybrid hydrogels<sup>58</sup>. A related four-arm PEG molecule, now terminated with four *N*-hydroxysuccinimide esters, can condense with an RLP bearing a single primary amine on the carboxy-terminal Lys and a secondary amine on the amino terminus<sup>59</sup>. End-crosslinking these amines affords a hydrogel with well-defined resilient networks that yield elastic recovery as high as 94%, even at a strain of 600%.

Besides RLP-based hydrogels, non-protein hydrogels have also been designed to mimic the mechanical properties of resilin. To closely mimic resilin, it can be advantageous to develop uniform chemical networks with multi-arm or micellar crosslinkers (FIG. 2c). Telechelic norbornene-functionalized hydrophilic PEG and hydrophobic poly(dimethylsiloxane) with a multi-arm crosslinker were used in photoinitiated thiol–ene click reactions to give homogeneous networks that afford hydrogels with resilience greater than 97% at strains of up to 300%<sup>60</sup>. A distinct strategy is micellar crosslinking copolymerization, in which block copolymers and macromolecular surfactants, both of which can act as multifunctional crosslinkers, self-assemble into micelles that give highly stretchable and resilient hydrogels<sup>61–63</sup>. In the case of the surfactants being the crosslinkers<sup>62</sup>, the resulting hydrogel has a resilience of 96% at a strain of up to 400%. Although these hydrogels exhibit high resilience, their mechanical strength is low (less than 200 kPa), which motivated the inclusion of inorganic nanoclays and SiO<sub>2</sub> nanoparticles to produce hydrogels with substantially higher mechanical strength, albeit with lower resilience (less than 80%)<sup>64,65</sup>. Overall, balancing mechanical strength and resilience among these synthetic resilin-mimicking hydrogels remains a challenge for being competitive with the native protein.

If we instead consider rubbers, when crosslinked they possess high stretchability, high elasticity, low elastic modulus and relatively high strength<sup>66</sup>. However, their resilience (less than 80%) is much lower than that of resilin, largely due to the random nature of their networks and appreciable intermolecular friction in dry rubbers. To address this, one can use cellulose as a biobased multifunctional initiator and crosslinker to prepare elastomers with well-defined networks, high resilience and high strength<sup>67</sup>. Thus, crosslinked cellulose-*graft*-polyisoprene elastomers were synthesized by combining atom transfer radical polymerization

and atom transfer radical coupling. To further increase the resilience of these elastomers, low molecular weight mineral oil was added as a lubricant, mimicking the hydrated state of resilin and lowering intermolecular friction in materials, which eventually have more than 98% resilience. In another approach, soybean oil-derived

resilient elastomers could be prepared without the addition of small molecular lubricants<sup>68</sup>. Here, acrylic polymers with unsaturated fatty acid side groups were decorated with furan groups, which can be crosslinked through Diels–Alder reactions with bis(dienophile) species (FIG. 2d). The self-lubricating effect of long fatty acid side chains act as internal plasticizers, endowing elastomers with high resilience.

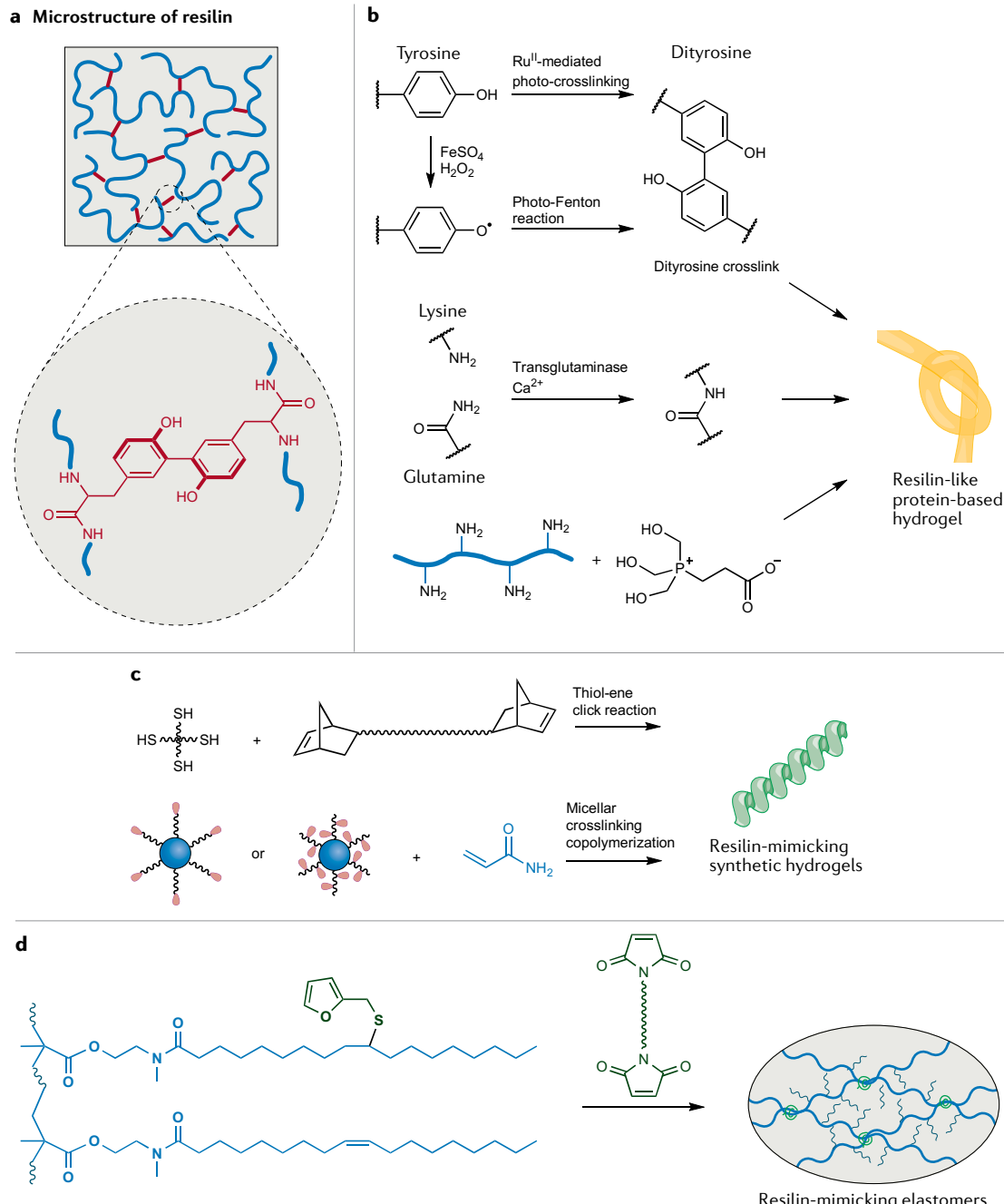


**Fig. 2 | Chemical approaches in the design of resilin-mimicking materials.** **a** The outstanding mechanical properties of resilin originate from its unique microstructure<sup>45</sup>. Long and flexible polymer chains, well-defined chemical networks and low intermolecular friction result in high resilience. **b** Crosslinking resilin-like proteins can be products of  $\text{Ru}^{\text{II}}$ -mediated photocrosslinking, the photo-Fenton reaction, a transglutaminase-catalysed reaction and Mannich-type reaction to give hydrogels<sup>55,57,228</sup>. Due to the specific crosslinking chemistry and hydration state, these protein-based hydrogels exhibit high resilience. **c** Bioinspired non-protein resilin-mimicking hydrogels can be prepared by a thiol-ene click reaction or micellar crosslinking copolymerization<sup>60,61,64</sup>. **d** Plant oil-based elastomeric resilin mimics can be converted into well-defined networks by Diels–Alder crosslinking of furan and maleimide groups<sup>67,68</sup>. The fatty acid side chains act as internal plasticizers, endowing elastomers with high resilience.

Table 1 | Mechanical parameters of resilin and resilin-mimicking materials

Protein/polymer	Crosslinks	Resilience (%)	Strength (MPa)	Extensibility (%)
Resilin	—	>95	>1	190
Resilin-like polypeptides	Tyr–Tyr <sup>53,55,56</sup>	92–97.7	0.07–0.1	277–600
	Lys–Gln <sup>228</sup>			
	Lys–HMP <sup>57</sup>			
	Cys–vinyl <sup>58</sup>			
	Lys–NHS <sup>59</sup>			
Resilin-mimicking hydrogels	Thiol–vinyl <sup>60</sup>	80–97	0.02–1.75	300–2,829
	Reactive micellar crosslinks <sup>61–63</sup>			
	Inorganic nanoparticle crosslinks <sup>64,65</sup>			
Resilin-mimicking elastomers	Functionalized cellulose isoprene crosslinks <sup>67</sup>	93–98	0.8–1.1	50–180
	Furan–maleimide <sup>68</sup>			

HMP, hydroxymethylphosphine; NHS, N-hydroxysuccinimide.

side chains gave dry elastomers with 93% resilience and tensile strength of 0.8 MPa.

The separate classes of resilin-mimicking materials have different advantages and disadvantages (TABLE 1). Although the hydrogels are very resilient, most have much lower tensile strength than resilin, which is better mimicked by the elastomers. As described above, a network of chemical crosslinks is the most crucial structural motif to afford high elastic recovery. Investigations of well-defined chemical networks are prevalent in the literature, yet there are few reports describing how to rationally design a well-defined structure. Previous work has highlighted the challenge of lowering intermolecular friction while maintaining sufficient mechanical strength. Innovative crosslinking chemistries will be needed to synthesize tougher and more elastic chemical networks. Tuning the size of crosslinking junctions may play an important role in enhancing mechanical strength. An optimal balance between the size and the crosslinking density can presumably enable high resilience and high mechanical strength. Moreover, due to the sequence nature of chemical components in resilin, hierarchical structures such as  $\alpha$ -helices and  $\beta$ -turns contribute to the strength and reversible energy storage. Thus, synthetic polymers with hierarchical structures are essential for advancing high-performance resilin-mimicking materials.

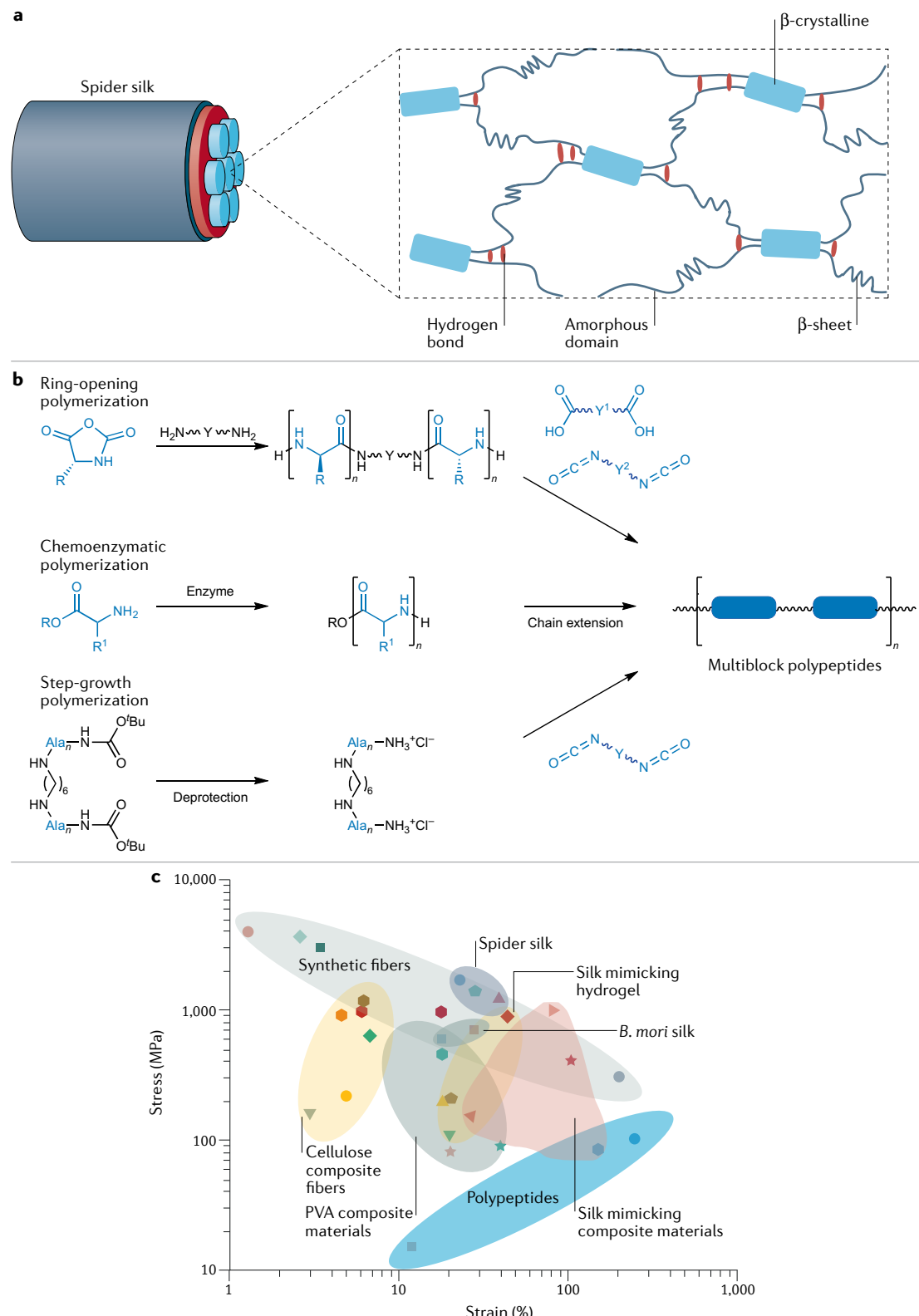
**Spider silk mimics.** Spider silks comprise high-performance synthetic fibres that many wish to mimic with synthetic materials. The native materials display fascinating mechanical properties because of their unique hierarchical structures, which feature crystalline  $\beta$ -sheet domains dispersed in an amorphous matrix<sup>69</sup> (FIG. 3a). The crystalline domains consist predominantly of a defined sequence of hydrogen bonds involving Gly and Ala residues that augment mechanical strength. The amorphous matrix is composed of Gly and other amino acid residues with bulky side chains. Notably, the Gly

residues induce the formation of helical structures and  $\beta$ -turns in an amorphous matrix<sup>70</sup> that is mainly responsible for the elasticity of spider silks<sup>71</sup>. In addition, spider silks undergo supercontraction at high humidity, which is rarely observed in synthetic fibres<sup>72</sup>. Various synthetic methods exist for spider silk mimics, with the most common approach being the biochemical spinning of proteins into fibres<sup>73,74</sup>. However, many challenges must be addressed before the large-scale production and application of protein fibres becomes possible.

We now introduce chemical and biochemical approaches that have afforded interesting silk-mimicking materials of late. Chemical designs focus on mimicking the hard  $\beta$ -sheet domains using hydrogen bond-rich peptides in a soft matrix of amorphous polymers. The most common strategy is to prepare multiblock copolymers by combining controlled polymerization towards independent segments with subsequent coupling reactions for chain extension (FIG. 3b). Thus, hard crystalline domains facilitate high strength, while the amorphous polymer chains offer toughness and elasticity. Another approach is to design synthetic hydrogels with hierarchical supramolecular structures, a method that has afforded a few outstanding artificial spider silks. Lastly, the preparation of composite materials is more prevalent in achieving high toughness and high strength.

Multiblock copolymers are well-explored materials for silk mimics. We present a few synthetic examples to illustrate the diversity of their chemical compositions. For example, the preparation of spider silk-mimicking materials from amino acids or polypeptides is largely targeted at the formation of crystalline  $\beta$ -sheet domains<sup>75</sup> (FIG. 3b). For example, rigid  $\beta$ -sheet-mimicking polyalanines were synthesized by anionic ring-opening polymerization of poly(ethylene glycol) diamine and *N*-carboxyanhydride derivatives of amino acids<sup>76</sup>. Further coupling reactions led to the formation of multiblock copolymers, wherein flexible non-peptide blocks replace the amorphous segments for aggregation into a soft matrix. Multiblock copolymers containing Ala<sub>4</sub> and GAGA sequences can undergo aggregation into  $\beta$ -sheet conformations in the solid state<sup>77</sup>. These copolymers can be further combined with polyalanine and polyisoprene using simple coupling reactions<sup>78</sup>, and polypeptides can be used in all segments of multiblock copolymers. In another work, multiblock polypeptides can have structures resembling natural spider silk proteins<sup>79</sup>. Two types of oligopeptides with sequences similar to those of spider silk proteins have been made by chemo-enzymatic polymerization. Multiblock polypeptides with polyalanine as a hard block and poly(glycine-*ran*-leucine) as a soft block were obtained by post-polycondensation between the oligopeptides. However, most of the above-mentioned studies do not include a direct comparison of the mechanical properties of the new mimics with those of spider silks.

Amine-terminated polypeptides of the form poly( $\gamma$ -benzyl-L-glutamate) have been synthesized by ring-opening polymerization and studied as spider silk mimics<sup>80</sup>. The amine groups condense with isocyanate-terminated polyurethane to enable chain extension into multiblock copolymers. The secondary



structures including  $\beta$ -crystalline domains and  $\alpha$ -helices can be obtained by controlling the average degree of polymerization of poly( $\gamma$ -benzyl-L-glutamate). Although the tensile strain reported was seemingly too large for silk-mimicking applications, the resultant pseudo-protein-like multiblock copolymer fibres exhibit high strength ( $\sim 100$  MPa) and impressive

toughness ( $\sim 387 \pm 35$  MJ m $^{-3}$ ). Polypeptides can also be used as silk mimics by the guided assembly of  $\beta$ -sheets into an amorphous network that accurately mimics the native microstructure. A 'grafting from' approach incorporated  $\beta$ -sheet-forming polypeptides into a 3D amorphous network<sup>81</sup>. Radical copolymerization of amine-containing acrylic monomers yielded an initial

◀ Fig. 3 | **Synthetic spider silk mimics recapitulate the primary or secondary structure of spider silk proteins.** **a** | The secondary structure of spider silks exemplifies how nano-sized crystalline  $\beta$ -sheets and hydrogen bonds in an amorphous matrix can endow a material with outstanding mechanical properties<sup>69</sup>. **b** | Spider silk-mimicking multiblock copolymers with amino acid derivatives can be prepared by ring-opening polymerization, chemo-enzymatic polymerization with subsequent chain extension or step-growth polymerization<sup>77–79</sup>. **c** | An Ashby plot of tensile stress versus strain for natural spider silks and synthetic mimics.

network of a hydrogel with pendant amine groups, which were used as sites for spatially controlled growth of polyvaline and poly(valine-*ran*-glycine) through *N*-carboxyanhydride-based ring-opening polymerization to give  $\beta$ -sheet nanocrystals. Overall, one of the most important challenges is to incorporate  $\beta$ -sheet structural mimics into synthetic polymers. Additionally, high molecular weight multiblock copolymers are non-trivial to make but are essential for achieving desired properties.

Along with polypeptides, supramolecular hydrogel fibres have also been used to mimic spider silks. This motivated the synthesis, for example, of a dynamic supramolecular polymer–colloidal hydrogel<sup>82</sup>, which was constructed with host–guest interactions between cucurbit[8]uril and methyl viologen (which together can afford a pseudorotaxane) attached from polymer-grafted  $\text{SiO}_2$  nanoparticles as well as naphthalene grafted from hydroxyethyl cellulose. By drawing this supramolecular hydrogel into filaments, the  $\text{SiO}_2$ -containing fibres have high tensile strength ( $193 \pm 54$  MPa) at reasonable strain ( $18.1 \pm 5.7\%$ ). The hydrogel was further developed into a supercontractile fibre that mimics spider silk<sup>83</sup>. Based on the first hydrogel network involving the above-mentioned supramolecular interactions, the hydrogel composite was imparted with the second network of covalent crosslinks, in which naphthalene-containing hydroxyethyl cellulose was functionalized with methacrylic anhydride to undergo UV light-triggered crosslinking. The resultant fibre, when subjected to high humidity, contracted by up to 50% of its original length — a value comparable to that of spider silk. In another study<sup>84</sup>, a hydrogel consisting of poly(acrylic acid) crosslinked with vinyl-functionalized  $\text{SiO}_2$  nanoparticles was processed into hierarchical core-sheath fibres, which were reinforced by metal ion doping and topological insertion of twists. As expected, introducing inorganic components such as  $\text{SiO}_2$  and metal ions afforded fibres with a tensile strength of 895 MPa and a stretchability of 44.3%, with both values approaching those for spider silk. In these synthetic hydrogel systems,  $\text{SiO}_2$  nanoparticles act like  $\beta$ -sheets, chemically crosslinking the amorphous polymer chains through supramolecular interactions such as electrostatic attraction and host–guest interactions.

Composite fibres are another class of desirable spider silk mimics. One of many possible approaches is to combine a polymer such as poly(vinyl alcohol) (PVA) with species such as graphene oxide quantum dots (GODs), which form  $\beta$ -sheet-like crystals<sup>85</sup>. This GOD-reinforced PVA composite film has a high tensile strength (152.5 MPa), in part because PVA is a useful semi-amorphous polymer matrix with extensive

hydrogen-bonding interactions similar to the native proteins. The surfaces and edges of each chemically oxidized GOD contain abundant hydroxy groups, epoxide and carboxyl groups that form multiple hydrogen bonds with PVA to effectively crosslink the chains. In a related inorganic approach, replacing the GODs with hydroxyapatite nanocrystals<sup>86</sup> gave fibres with markedly high tensile strength (949 MPa), toughness ( $429 \text{ MJ m}^{-3}$ ) and ductility (80.6%).

Biomimetic composites have recently been combined with sustainable natural resources<sup>87,88</sup>. For example, biomass-derived lignosulfonic acid (a lignin-based polyanionic macromolecule when in its basic form) can be interspersed in a PVA matrix<sup>87</sup>. Another strategy towards sustainable supramolecular polymers is the topological confinement of PVA in tannic acid, a naturally occurring dendritic polyphenol that offers a high density of hydrogen bonds<sup>88</sup>. Tannic acid–PVA composites consisting of interpenetrating 3D supramolecular clusters have a toughness of  $\sim 395.2 \text{ MJ m}^{-3}$  with tensile strength of  $\sim 104.2$  MPa and strains in excess of 400%.

While much progress has been made recently (FIG. 3c), no synthetic materials have matched spider silk's tensile strength of 1 GPa and maximum elongation of 20–40%. Some reports of toughness can be misleading because they describe materials with a very large tensile strain (these materials should instead be called 'high elastomers'). Mimicking spider silks with all-organic polymers remains challenging, but the success of composites containing inorganic fillers may inspire the design of all-organic polymer composites with comparable or higher performance. These might feature organic fillers such as cellulose nanocrystals (CNCs), which have rarely been explored in terms of mimicking silk materials<sup>89</sup>. Precision chemical approaches are crucial to controlling the interface between fillers and matrices and the dynamic matrix networks. A hybrid of physical (crystalline domains) and chemical interactions could serve as a promising alternative to tackle this complex challenge.

### Adaptive polymeric materials

An intriguing feature of biological materials is their ability to respond to external or internal stimuli by appropriately altering their physicochemical properties. Rational design of topological architectures and responsive building blocks allows the exploration of polymers that respond to environmental changes such as pH, temperature, light, ionic strength, mechanical force and magnetic/electric fields. The stimuli can cause changes in macroscopic properties such as colour, shape, stiffness and volume<sup>90–93</sup>. Responsive polymer systems are useful for 'smart' applications, including drug delivery, sensors, optical systems, textiles and electromechanical systems<sup>90</sup>. Chemical modification of biobased polymers can be used to generate bioinspired stimulus-responsive materials with unique properties<sup>94</sup>. For example, chitin in crustacean shells can be basified and converted into chitosan, a linear polysaccharide whose pendant amines are sensitive to pH and affect macroscopic properties such as aqueous solubility (soluble at low pH and insoluble at high pH)<sup>95</sup>. In another example, CNCs are physically and optically adaptive with customized surface

modifications that trigger responses to stimuli<sup>96</sup>. Owing to high H<sub>2</sub>O content, ambient sensitivity to stimuli, exceptional biocompatibility and tunable architectures that mimic biological tissues, hydrogels provide a ubiquitous platform from which to develop bioinspired stimulus-responsive materials<sup>97</sup>. In addition, biomimetic adaptive materials are conceived as block copolymer thin films, fibres, nanoparticles and hybrid composites. To bridge recent advances in these areas to biomimetic and bioinspired systems, we discuss mechanically and optically adaptive materials.

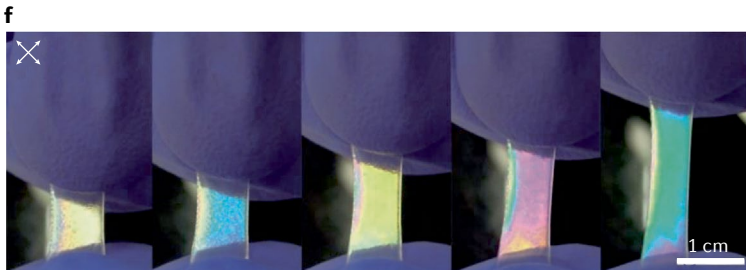
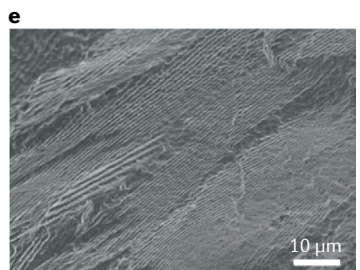
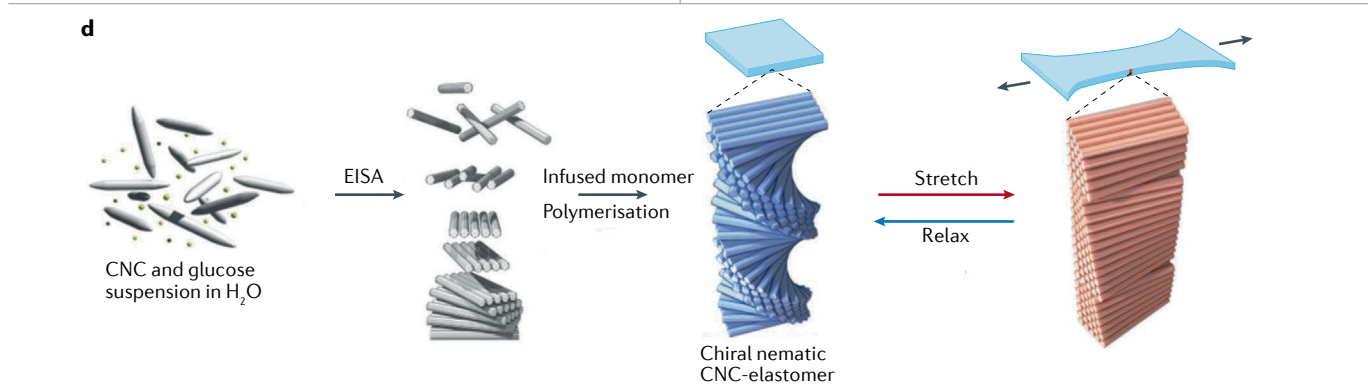
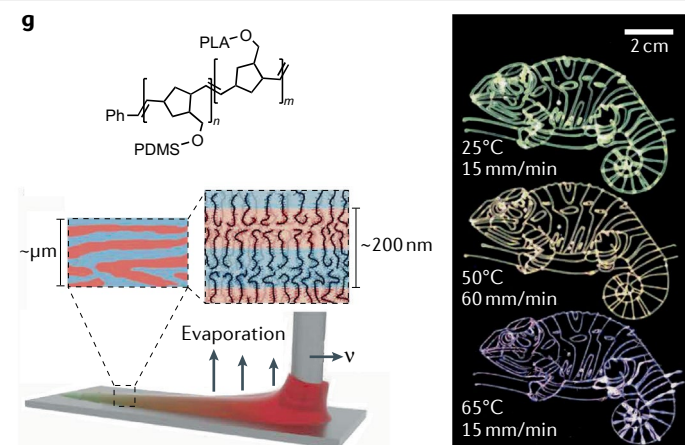
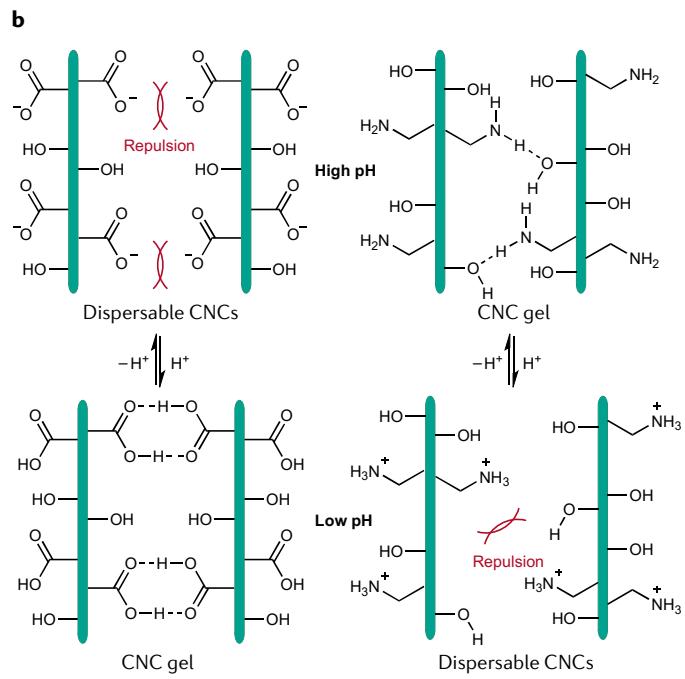
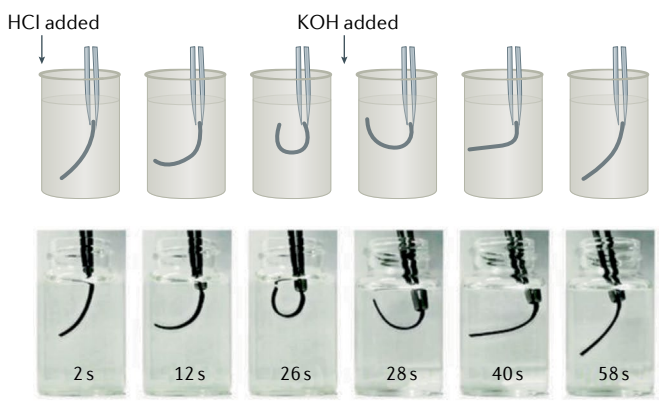
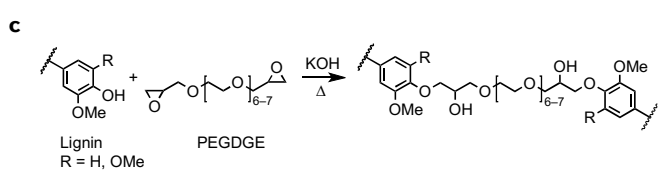
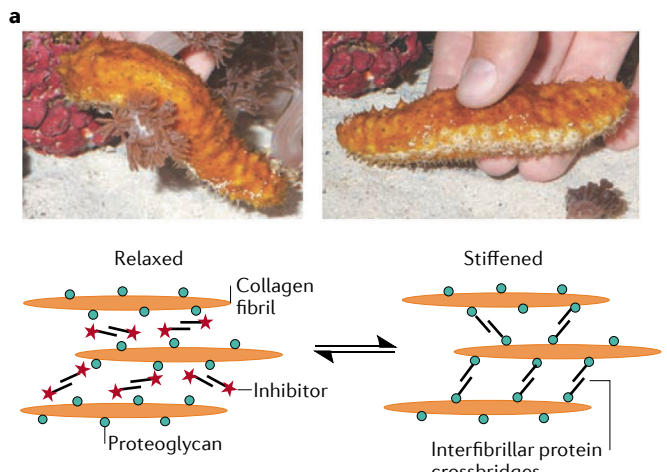
**Mechanically adaptive polymer composites.** Polymeric materials that experience reversible changes in mechanical properties on exposure to stimuli are attractive for the design of smart materials<sup>4</sup>. The stiffening of sea cucumbers, plant guard cell control of stomas and pinecone opening are natural ‘morphing’ phenomena that have inspired the development of mechanically adaptive biomimetic and bioinspired materials<sup>98</sup>. Echinoderms such as starfish and sea cucumbers can rapidly and reversibly alter the stiffness of their body walls<sup>9,99,100</sup> (FIG. 4a). In these organisms, the mutable collagenous tissue (also called ‘catch connective tissue’) is controlled by the nervous system, which can rapidly and dynamically change the mechanical properties to allow complex motions in feeding, defence, reproduction and posture<sup>101</sup>. Mutable collagenous tissue consists of high aspect ratio collagen fibrils embedded in a viscoelastic interfibrillar matrix, which can be considered a hydrated gel incorporating interfibrillar proteins (tensilin, stiparin, softenin and fibrosurfin) and other components responsible for interfibrillar cohesion<sup>102</sup>. On exposure to stimuli, juxtaligamental cells within the tissue release proteins, which in seconds alter interfibrillar binding (including crosslinking and uncrosslinking of the interfibrillar matrix) to switch between stiff and soft states, respectively<sup>101</sup>. The attached proteoglycans on collagen fibrils serve as binding sites for interfibrillar cohesion mediated by crosslinker proteins such as stiparin and tensilin. Increasing interfibrillar cohesion leads to nearly a 50-fold increase in fibrillar stress in the stiff state, such that mutable collagenous tissue serves as a blueprint for mechanically adaptive bioinspired structural materials. The following sections describe bioinspired biobased systems that incorporate features of mechanical adaptability.

Hydrolysis of cellulose fibres composed of β-1,4-linked anhydro-D-glucose chains afford rigid biobased rod-like nanomaterials with unique properties that can mimic stiffness-changing biomaterials<sup>96</sup>. Depending on the hydrolysis conditions, CNCs can have high aspect ratios (greater than 10) and a range of lengths (50–1160 nm) and diameters (3–70 nm)<sup>103</sup>. In addition, CNCs have a high surface area (~250 m<sup>2</sup> g<sup>-1</sup>), high tensile strength (7.5 GPa), high stiffness (Young’s modulus ~105–143 GPa) and low density (~1.61 g cm<sup>-3</sup>)<sup>96,103</sup>. Reactive hydroxy groups on the surface of CNCs open vast opportunities for surface modifications. Chemoresponsive and mechanically adaptive composites have been designed by incorporating CNCs into a poly(ethylene oxide-*co*-epichlorohydrin) or PVA matrix<sup>9,104</sup>.

**Fig. 4 | Preparation and chemistry of biomimetic stimulus-responsive polymer composites.** **a** | Sea cucumbers can switch between relaxed and stiffened states because of their mutable collagenous tissue<sup>9</sup>. In simple terms, the stiffness-changing behaviour involves spindle-shaped collagen fibrils, which are discontinuous parallel aggregates<sup>102</sup>. Proteoglycans bind proteins such as stiparin and tensilin, which bridge the fibrils. **b** | Amine- or carboxy-functionalized cellulose nanocrystal (CNC) suspensions have a pH-dependent stiffness that depends on attractive hydrogen bonds or electrostatic repulsions<sup>105</sup>. **c** | Lignin-based pH-responsive reversible actuators<sup>114</sup>. **d** | A stretchable chiral nematic CNC–elastomer composite can be prepared by evaporation-induced self-assembly (EISA)<sup>122</sup>. **e** | A cross-section scanning electron micrograph of the CNC–elastomer film shows periodic structures. **f** | Photographs of CNC–elastomer samples viewed under crossed polarizers while stretched. **g** | Direct-write chameleon patterns can be generated under constant 3D printing conditions<sup>143</sup>. Printing speed *v* and substrate temperature can control on-the-fly tuning of photonic properties. PDMS, poly(dimethylsiloxane); PEGDGE, poly(ethylene glycol) diglycidyl ether; PLA, poly(lactic acid). Part **a** adapted with permission from REF.<sup>9</sup>, AAAS and REF.<sup>102</sup>, Springer Nature Limited. Part **b** adapted with permission from REF.<sup>105</sup>, ACS. Part **c** adapted with permission from REF.<sup>114</sup>, ACS. Part **d**, **e**, and **f** are reprinted from REF.<sup>122</sup>, CC BY 4.0. Part **g** adapted with permission from REF.<sup>143</sup>, AAAS.

Competitive hydrogen bonding within the matrix polymers and CNCs result in adaptable stiffening properties. Functionalizing the CNC surface with carboxylic acid or amine moieties confers pH-responsive behaviour, with the material transitioning from an aqueous dispersion to a hydrogel at higher pH<sup>105</sup> (FIG. 4b). Indeed, at lower pH, electrostatic repulsions between the ammonium moieties inhibit aggregation, while at higher pH, the attractive hydrogen-bonding forces dominate. Inspired by muscle expansion and contraction through the combination and separation of Ca<sup>2+</sup> ions and troponin in sarcoplasm, reversible ion exchange was used to enable cellulose hydrogels to exist in different mechanical states (fluid, brittle and rigid)<sup>106</sup>. The hydroxy groups in cellulose coordinate metal ions, such that high Ca<sup>2+</sup> concentration favours the adoption of a crosslinked network (compressive strength ~2.2 MPa), while high Zn<sup>2+</sup> concentration eliminates the intermolecular connections between cellulose, resulting in a fluid state.

For stiffness-changing polymer composites, the importance of hydrophobic polymer matrices stands out. Although mixing a hydrophilic polymer matrix with hydrophilic CNCs in aqueous solution is convenient, these polymer composites are often mechanically weak in the hydrated states due to the competitive hydrogen bonding of H<sub>2</sub>O molecules. This motivated the development of nanocomposites with a tunable tensile storage modulus based on H<sub>2</sub>O-triggered changes<sup>107</sup>. The CNC composites were prepared by a template approach based on hydrophobic poly(styrene-*co*-butadiene) (SBR) and polybutadiene matrices. In the dry state, incorporation of tunicate CNC nanofillers (ground shells of sea squirts) offers substantial reinforcement. For example, SBR with 17% nanofiller has a storage modulus of 236 MPa



compared with that of neat SBR of  $\sim$ 1 MPa. However, interactions between the template and the hydrophobic polymer were still relatively weak, resulting in a dramatic decrease in wet strength (39 MPa for wet SBR with 17% nanofiller) of these polymer composites. Further refinements are required to improve interfacial properties of hydrophobic polymers and CNCs. A new supramolecular approach combined CNCs with plant-oil-based thermoplastic polymers<sup>108</sup>, in which the compatibility between the two constituents was improved by tuning interfacial interactions. Thus, unsaturated fatty acid side chains in the polymers were modified with hydroxy and carboxyl groups, facilitating hydrogen bonds with CNCs, with the resulting supramolecular nanocomposites exhibiting  $\text{H}_2\text{O}$ -triggered stiffness-changing behaviour. Further optimization of the functional groups with epoxide units caused the nanocomposites to show  $\text{H}_2\text{O}$ -triggered stiffness changes, while keeping the wet tensile strength at  $\sim$ 20 MPa (with 50 wt% CNCs)<sup>109</sup>. The reduction of mechanical strength was only 59%.

We have yet to describe lignin, which is among the most abundant biomass forms and has rich chemical functionalities, reinforcing properties, antioxidant strength and UV-blocking abilities. These traits make it a useful substrate for sustainable and bioinspired material design<sup>110,111</sup> and one of the most appealing renewable polymers capable of stimulus-responsive behaviour due to its unique polyphenolic structures<sup>112</sup>. Electrospun blends of kraft lignin fractions have been investigated as moisture-responsive films with reversible shape changes<sup>113</sup>. Intrinsic differences in the thermal flow behaviour of solvent-fractionated lignin were used during controlled thermal treatment of electrospun fibres. In another investigation, lignin-based pH-responsive hydrogels were developed by a one-step crosslinking reaction of industrial kraft lignin with poly(ethylene glycol) diglycidyl ether<sup>114</sup> (FIG. 4c). These hydrogels are reversibly formed between softening and enhancement and between straight and bending shapes depending on the pH. This behaviour arises due to the protonation and charging of lignin structures.

In general, mechanically adaptive materials are less widely explored than the protein-mimicking and self-healing materials we describe in the next section. Complex molecular-level interactions require materials to change their mechanical properties in response to the environment. As described already, there are many natural systems with such features that have inspired synthetic systems as biomimetic and bioinspired adaptive materials. Recent efforts have afforded more sustainable stiffness-changing materials derived from natural biomass. Nevertheless, further refinements are required for better interfacial properties both in the dry state and in the wet state to maintain useful mechanical properties. It is expected that more attention will be given to cellulose nanofibres, which possess higher aspect ratios than CNCs.

**Optically adaptive polymers.** Animals and plants have evolved complex molecules and materials to exhibit vibrant colours<sup>115,116</sup>. Colour has become a feature for many evolutionary functions, including defence,

signalling, mimicry and reproduction. Biological colouration provides a dynamic form of information, where the colours change over various timescales when an organism encounters stimuli. Well-known examples include the rapid colour changes of cephalopods and chameleons used for camouflaging as well as beetles responding to humidity. Organisms can express pigmentary and/or structural colouration, with the mechanisms being quite distinct. Pigments such as melanins, carotenoids and porphyrins are widespread in nature and absorb light of specific wavelengths, while reflecting others<sup>117</sup>. In contrast, visible light interference with (typically 100 nm or larger) periodic domains such as diffraction gratings and photonic crystals establishes structural colours<sup>118</sup>. Constructive interference of these periodic features leads to intense structural colours dictated by Bragg's law. The colour-changing properties of chameleons result from the active tuning of a lattice of guanine nanocrystals within a thick superficial dermal layer<sup>119</sup>, with the wavelength of reflected light dependent on the refractive indices and periodicities of the materials within the structure<sup>120</sup>. Artificial photonic materials are commonly prepared from monodisperse colloidal particles. Polymeric materials are well suited as environmentally triggered colour-changing materials due to their ability to change their refractive index and periodicity of photonic structures upon exposure to a stimulus. Developing adaptive or stimulus-responsive structural colour materials requires further refinements since the refractive index or periodicity should be altered in response to a stimulus, such as humidity, temperature, pH, strain or light. Adaptive colouration has potential applications in defence, smart sensors, smart windows, intelligent textiles, wearable devices and displays, to name a few. Naturally occurring polymers such as cellulose, chitin, keratin and silk proteins provide the building blocks for biobased structural colour materials<sup>121</sup>. With these building blocks at hand, strategies including lithography, imprinting, evaporation-driven assembly, self-assembly, force-induced alignment and layer-by-layer assembly have been explored to fabricate structural colour materials<sup>121</sup>. We now discuss examples of biobased approaches towards attaining optically adaptive structural colour materials.

CNCs are chiral due to the D-glucose units in cellulose and can undergo evaporation-induced self-assembly to give chiral nematic (cholesteric) liquid crystals, which have a left-handed helical structure<sup>103</sup>. These chiral nematic structures can diffract light, leading to an iridescent appearance when the pitch of the helix is comparable to the wavelength of visible light<sup>122,123</sup>. CNCs have been used to make photonic materials either by helical organization of the chiral nematic liquid crystalline phase or by using templates from the chiral nematic structure<sup>124,125</sup>. CNCs behave as lyotropic liquid crystals, which, when present above a critical concentration, convert into a liquid crystalline phase. This anisotropic chiral nematic structure can be preserved in the solid state.

The desirable photonic properties of CNC-containing films have motivated the development of different forms. Typically, nematic films of CNCs can be made by drying aqueous suspensions, with variables such as ionic

strength, temperature, time and surface influencing self-assembly. Additives, including glucose, NaCl and ionic liquids, can alter optical properties by causing red and blue shifts. Alternatively, incorporating PEG into CNC suspensions afforded flexible humidity-responsive chiral nematic composites<sup>124</sup>. Tunable structural colours across the entire visible spectrum are available by adjusting the CNC-to-PEG molar ratio and by changing the relative humidity. Use of glycerol as the additive achieved similar behaviour<sup>126</sup>. Dynamic optical properties can be obtained by incorporating photonic crystals into elastomers, as inspired by the elastic skin of a chameleon<sup>127</sup>. Indeed, stretchable CNC-elastomer composites with a chiral nematic organization of CNCs exist<sup>122,128</sup>, but phase separation of hydrophobic monomers during evaporation-induced self-assembly of CNCs is a challenge when one prepares homogeneous elastomeric composite films. To overcome this, a glucose–CNC film can first be prepared by evaporation-induced self-assembly, swelled with  $\text{Me}_2\text{SO}$  and impregnated with ethyl acrylate and 2-hydroxyethyl acrylate. These monomers undergo radical polymerization to afford highly stretchable CNC–elastomer composites that can experience more than 900% elongation (FIG. 4d). The reversible conformation change of the chiral nematic CNCs between a chiral nematic arrangement and a pseudo-nematic arrangement resulted in films with periodic structures (FIG. 4e) that give vivid interference colours on stretching or relaxation (FIG. 4f).

Fibroin-derived silk inverse opals (SIOs) are 3D photonic crystals that display vivid structural colours due to periodic lattice voids that periodically modulate the refractive index<sup>129,130</sup>. Silk fibroin can be dissolved in aqueous electrolytes, such as LiBr, where it self-assembles into elongated nanofibrils<sup>131</sup>. SIOs are also accessible through template-assisted interfacial self-assembly, where a 3D poly(methyl methacrylate)<sup>132</sup> or polystyrene<sup>133</sup> colloidal template is infiltrated with regenerated silk solution. Self-assembly through solvent evaporation and removal of the colloidal spheres by chemical etching or calcination leaves SIOs with vivid structural colours due to the light diffraction induced by the structural periodicity. SIOs are elastic and can withstand and recover from compressive loads through reversible pore deformation<sup>134</sup>. In addition, they are superhydrophobic due to their nanoscale surface texture. Reconfigurable and responsive optical materials can be developed using SIOs owing to their controllable conformational changes on exposure to  $\text{H}_2\text{O}$  vapour or UV light<sup>133</sup>. Tunable structural colour in a mechanically flexible and controllable format has been achieved with naturally derived silk fibroin-based photonic crystal superlattices with multiple stacking orders and lattice periods<sup>135</sup>.

In addition to biobased composites, it is possible to use a block copolymer (BCP) as a precursor to bioinspired photonic crystals. Through precision control of composition and molecular structure, BCPs undergo microphase separation into nanostructures such as spheres, cylinders, gyroids and lamellae, with the last being suitable for developing Bragg mirror-type photonic structures. The nanostructure formation is

governed by molecular weight, block ratio and structural dissimilarity. Since the refractive index of polymers is around 1.5, the underlying periodic structures require dimensions greater than 100 nm to have visible-light photonic properties<sup>136</sup>. To develop such periodicity, the first intuitive approach is to make ultra-high molecular weight (UHMW) BCPs with a narrowly dispersed distribution centred at 1 MDa or higher. Controlled radical polymerization and anionic polymerization can afford such BCPs, with living anionic copolymerization giving 1–2-MDa poly(4-methylstyrene)-*block*-polyisoprene<sup>136</sup>. Microphase separation for the UHMW BCPs in the bulk state affords well-ordered lamellar and spherical domains with large domains (100–200 nm). The high order of the underlying domains and the different refractive indices of the block segments produced vivid structural colours. In another approach, UHMW BCPs self-assemble in organic solvents to give micellar photonic crystals<sup>137</sup>. Furthermore, polymer blends can be used to broaden the domain spacing. A ternary BCP blend of 391 kDa polystyrene-*block*-polyisoprene copolymer, 13 kDa polystyrene and 13 kDa polyisoprene adopts a lamellar morphology with a periodicity of 140 nm (REF. <sup>138</sup>). This simple method demonstrates the ease with which large-area, tunable, highly reflective and flexible films can be fabricated from BCP-based materials.

Another promising class of materials for photonic crystal development is bottlebrush BCPs, which feature polymeric side chains grafted to a linear backbone<sup>139</sup>. The high branch-to-backbone ratio affords self-assembly properties that differ from those of linear polymers. With side chain lengths that have molecular weights below the entanglement threshold, adjacent side chains are sterically protected from one another due to congestion, even in the UHMW regime. Thus, bottlebrushes self-assemble much more quickly than linear polymers. In addition, the bottlebrush topology allows easy fabrication of large domains with extremely high molecular weights. Unlike linear BCPs, these UHMW bottlebrush BCPs can be rapidly prepared by ring-opening metathesis polymerization, which gives macromonomers that can be linked into brush BCPs. This ‘grafting-through-polymerization’ strategy affords highly uniform brush BCPs, where the sterically encumbered array of low molecular weight side chains substantially inhibits chain entanglement and forces the unifying main chain to assume a highly elongated conformation. Consequently, these brush BCPs rapidly self-assemble into stacked lamellae of alternating domain layers to ultimately give 1D photonic crystals<sup>140</sup>. By changing the rigidity of grafted side chains, brush BCPs can be engineered to reflect UV, visible and near-IR light. Bottlebrush BCPs have been prepared with a range of monomers, including lactide and *n*-butyl acrylate<sup>141</sup>, lactide and styrene<sup>142</sup>, and hexyl isocyanate and 4-phenylbutyl isocyanate<sup>140</sup>. More recently, an additive manufacturing direct-write 3D printing method was used to make bottlebrush BCP photonic crystals with a tunable structural colour and peak-reflected wavelength over the range from 403 to 626 nm (blue to red)<sup>143</sup>. In this case, a well-defined poly(dimethylsiloxane)-*block*-poly(lactic acid) was synthesized using a combination of anionic ring-opening polymerization and sequential

graft through ring-opening metathesis polymerization (FIG. 4g). During the 3D printing process, microphase separation and solvent evaporation occur simultaneously to form lamellae. Adjusting the applied pressure, printing speed and bed temperature can tune the optical properties of three separate chameleon patterns.

In summary, biobased materials offer advantages such as renewability, unique interfacial chemistry, desirable thermal properties and mechanical robustness to develop bioinspired photonic structures<sup>121</sup>. Various top-down and bottom-up fabrication approaches have been investigated, but the use of biobased chemicals to prepare optically adaptive materials can be challenging because natural products can have variable structures, yet precise orientations of nanoscale domains are necessary to make photonic structures. Biobased BCPs have not been substantially explored as adaptive photonic materials. One promising strategy is to prepare bottlebrush polymers using cellulose as a backbone and other biobased polymers as side chains. Although the synthetic foundation of the ‘grafting from’ strategy has been well established, the precise preparation of biobased BCPs with bottlebrush topologies remains a challenge.

**Biobased self-healing polymer materials.** Natural biomaterials can often spontaneously repair physical damage, which crucially increases the survival and lifetime of plants and animals. Inspired by biology, we have long pursued synthetic self-healing polymer materials that can improve product safety, increase service life, increase energy efficiency and reduce environmental impact<sup>144</sup>. For sustainable development, it is necessary to promote renewable and eco-friendly biobased materials with self-healing properties. We now consider self-healing polymer materials, especially those derived from common biobased components such as natural rubber<sup>145</sup>, plant oil<sup>146</sup>, cellulose<sup>147</sup> and furan<sup>148</sup>.

**Intrinsic self-healing polymers.** Self-healing materials can be divided into two main categories according to the healing mechanisms: extrinsic and intrinsic<sup>149</sup>. The former involves releasing healing agents in the crack areas by macroscopic or microvascular channels that trigger re-formation of polymer networks. However, extrinsic self-healing materials require the introduction of healing reagents, and the number of damage-healing cycles is thus limited. To overcome these drawbacks, intrinsic self-healing polymers with reversibly formed covalent linkages, such as disulfides<sup>150</sup>, imines<sup>151</sup>, boronate esters<sup>152</sup>, acylhydrazones<sup>153</sup> and (retro-)Diels–Alder adducts<sup>154</sup>, are intensively studied (FIG. 5a). In this section we discuss some recent progress on intrinsic self-healing polymers.

The Diels–Alder cycloaddition is one of the most versatile strategies to introduce dynamic covalent bonds into self-healing polymer materials. In a classic example, biobased polyesters with furan groups on the polymer main chain can be prepared and crosslinked with a bis(maleimide) to give self-healing materials<sup>148</sup> (FIG. 5b). Similarly, natural rubber modified with maleic anhydride and furfurylamine can undergo reversible crosslinking on heating, enabling self-healing behaviour<sup>154</sup>. In a more

convenient chemical route<sup>155</sup>, furfurylamine was grafted onto epoxidized natural rubber through a ring-opening reaction, which makes Diels–Alder chemistry apt for self-healing. This dynamic Diels–Alder chemistry has also proven efficient in the preparation of cellulose-based self-healing hydrogels<sup>156</sup>. Other reversible linkages used include disulfide bonds — a self-healing rubber can be made by simply tailoring the sulfur vulcanization procedure<sup>157</sup> — with UV irradiation accelerating disulfide metathesis and self-healing<sup>150</sup>. In other work, epoxidized natural rubber-based self-healing elastomers were prepared through transesterification of β-hydroxy ester linkages<sup>145</sup> (FIG. 5c). These epoxides are susceptible to attack from an aniline trimer, the presence of which confers elastomers with self-healing, recyclable and shape-memory properties.

Compared with dynamic covalent crosslinking, non-covalent networks are more easily constructed and incorporated into intrinsic self-healing biobased polymer materials. Plant oil-derived self-healing polymers were prepared to establish dynamic physical crosslinking using supramolecular interactions and hydrogen bonding formed by plant oil-derived methacrylate and poly(4-vinylpyridine)<sup>146</sup>. Similarly, semi-interpenetrating elastomers have been prepared by bulk radical polymerization of ethyl cellulose, furfural and fatty acid-derived monomers<sup>147</sup>. The strong hydrogen bonding offered by ethyl cellulose aids the self-healing shape-memory effect of these elastomers. In general, intrinsic self-healing polymer materials require more sophisticated treatments to undergo self-healing, which may limit their application. Thus, there is a strong need to develop self-healing polymer materials that can heal at ambient temperature without external stimuli.

**Autonomous self-healing polymers.** Among intrinsic self-healing polymers, autonomous self-healing polymers without external stimuli are the subject of intensive research<sup>158</sup>. Non-covalent interactions such as hydrogen bonding<sup>159</sup>, host–guest interactions<sup>160</sup>, metal–ligand coordination<sup>161</sup> and electrostatic interactions<sup>162</sup> have been used to design autonomous self-healing polymer materials. The high mobility of polymer chains at room temperature is a crucial prerequisite for autonomous self-healing.

Hydrogels are composed mainly of H<sub>2</sub>O, such that they have high chain mobility at room temperature. Polysaccharides such as cellulose and chitosan are widely used in self-healing hydrogels due to their renewability and extraordinary mechanical properties. Many autonomous self-healing hydrogels have been realized by using dynamic covalent and non-covalent bonds<sup>163,164</sup>. Thus, dynamic acylhydrazone linkages play a key role in cellulose-based self-healing hydrogels<sup>165</sup>. When the hydrogels crack, the macromolecules diffuse towards the damaged interface, re-forming the reversible acylhydrazone linkages for fast recovery (FIG. 5d). Polysaccharide can be prepared from aqueous solution chitosan and cellulose acetate<sup>166</sup>. Chitosan amino groups and the cellulose acetate carbonyl groups afford dynamic covalent amide bonds, enabling autonomous hydrogel healing. In terms of a hydrogen-bonding strategy, the

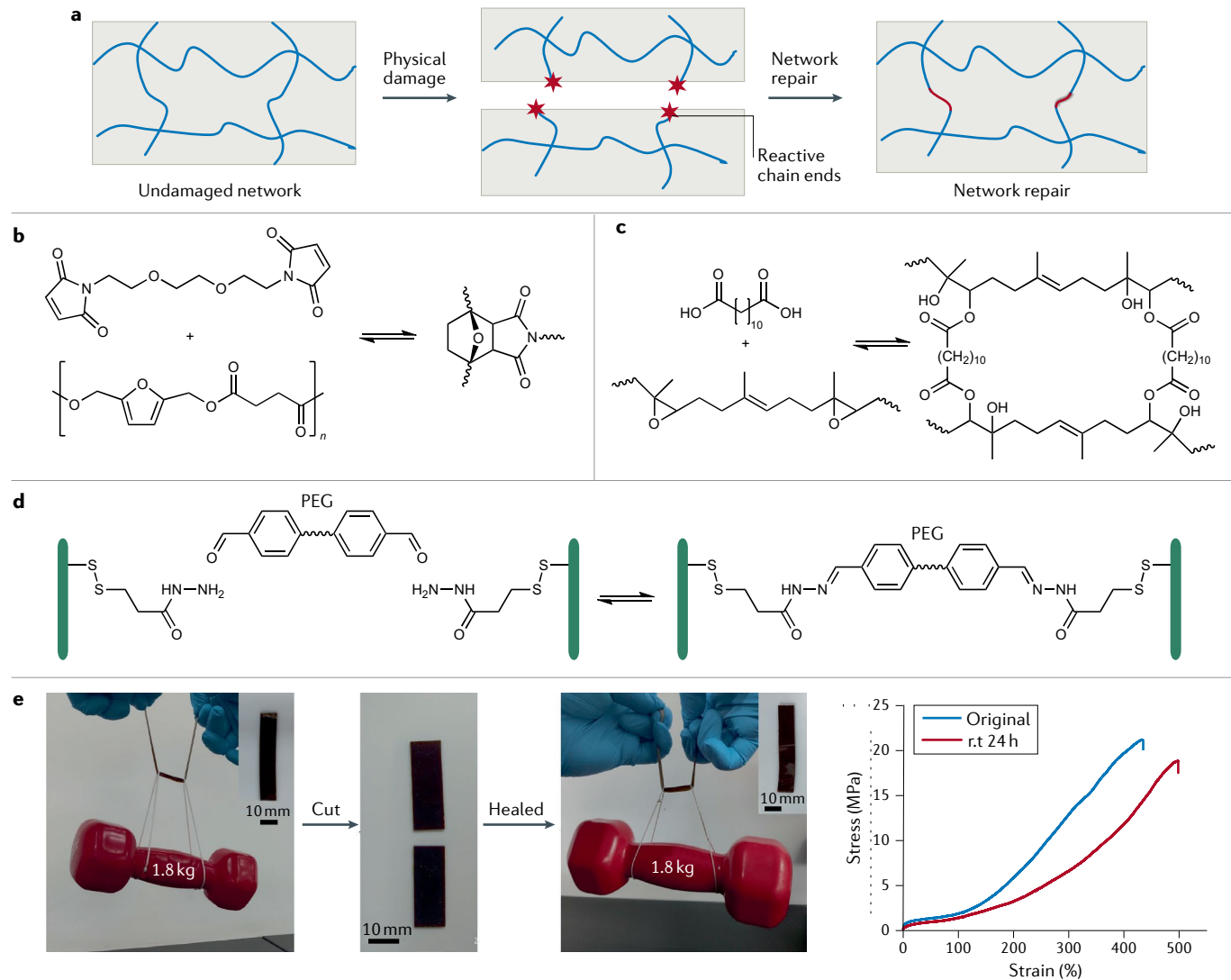


**Fig. 5 | Biobased elastomers and hydrogels with dynamic chemical networks can self-heal.** **a** Mechanical cleavage of polymer chains affords reactive end groups, but these can find each other to afford bond reconstruction and physical repair. **b** Biobased polyester elastomers with furans in their main chain participate in reversible Diels–Alder chemistry with maleimide groups to enable self-healing<sup>148</sup>. **c** Epoxidized natural rubber can be chemically crosslinked with an  $\alpha,\omega$ -diacid<sup>145</sup>. The  $\beta$ -hydroxy ester groups endow epoxidized natural rubber with self-healing properties. **d** Hydrogels based on carboxyethyl cellulose-*graft*-dithiodipropionate dihydrazide can be crosslinked with a poly(ethylene glycol) (PEG) derivative

bearing benzaldehydes at both ends<sup>51</sup>. The resulting covalent acylhydrazone linkages are dynamic, enabling the hydrogels to rapidly self-heal. **e** A castor oil-derived polyamide is an ultrastrong self-healing elastomer<sup>172</sup> that can be cut into two pieces and healed at room temperature (rt), after which 88% of tensile strength is recovered. Properties such as crystallinity, efficient chain entanglement, high hydrogen-bond density and olefin cross-metathesis in polyamide elastomers are responsible for strength and self-healing. Part **b** adapted with permission from REF<sup>148</sup>, ACS. Part **c** adapted with permission from REF<sup>145</sup>, ACS. Part **d** adapted with permission from REF<sup>165</sup>, Wiley. Part **e** adapted with permission from REF<sup>172</sup>, ACS.

large number of  $-\text{OH}$  and  $-\text{CO}_2\text{H}$  groups on cellulose could facilitate self-healing. A cellulose-based hydrogel can be obtained simply by immersing sodium carboxymethyl cellulose paste in citric acid solution<sup>167</sup>, with the product exhibiting room-temperature self-healing with ~80% efficiency. One of the most difficult issues for autonomous self-healing hydrogels is their low mechanical strength, which limits their applications<sup>163,168</sup>. To meet this challenge, a poly(acrylic acid)-based hydrogel was developed using  $\text{Fe}^{3+}$  ions and TEMPO-oxidized (TEMPO is (2,2,6,6-tetramethylpiperidin-1-yl)oxyl) cellulose nanofibres as crosslinkers, which led to materials with enhanced tensile strength (1.35 MPa) and healing

efficiency (90%)<sup>168</sup>. Furthermore, a method to prepare hydrogels based on  $\text{Fe}^{3+}$ -containing hydroxyethyl cellulose was explored<sup>169</sup>. In this system, hydrogen bonds and ion-dissipative coordination interactions are essential for high healing efficiency (87%) and high tensile strength (3.5 MPa).

Elastomers are widely used engineering materials, and their glass transition temperatures are typically below room temperature — ideal behaviour for autonomous self-healing materials. However, in the case of elastomers, mechanical strength and self-healing ability are often contradictory<sup>150</sup>. Strong bonds give a mechanically robust yet less dynamic system without

autonomous healing, while weak bonds help dynamic healing but produce relatively soft materials. Therefore, it is challenging to prepare mechanically strong autonomous self-healing elastomers. Research on autonomous self-healing elastomers is focused mainly on the balance of mechanical strength and self-healing efficiency. In one study, peroxide-initiated polymerization of zinc dimethacrylate in biobased natural rubber generated massive ionic crosslinks to give self-healing rubbers with a tensile stress of 0.7 MPa<sup>162</sup>. The ionic supramolecular network of natural rubber maintained good flexibility and mobility, facilitating self-healing at ambient temperature. Moreover, brominated natural rubber reacted with different amines, forming ionically crosslinked rubber with outstanding self-healing properties and tensile stress of 0.7 MPa<sup>170</sup>. Introducing cellulose and chitosan into natural rubber-based autonomous self-healing composites further increases the mechanical strength of the materials. The tensile strength of the composite elastomers increased to 1.9 MPa<sup>159,171</sup>. However, the mechanical strength of biobased autonomous self-healing elastomers is still too low for practical applications. To address this, a class of new polyamide elastomers was recently developed, and these materials combine multiple dynamic interactions, including efficient chain entanglement, hydrogen bonding and olefin cross-metathesis<sup>172</sup>. With the presence of nano-sized crystalline domains, these autonomous self-healing polyamide elastomers have tensile strengths as high as 20 MPa (FIG. 5e).

In summary, dynamic physical and chemical bonding is crucial to reliably produce a self-healing network. The recent focus has shifted to sustainable biobased materials. A clear target of what level of healing is sufficient, including property replication and healing kinetics, remains to be determined, as does the level of recyclability. The chemistry, especially the underlying thermodynamics and kinetics of specific reversible covalent and non-covalent interactions, ultimately dictates macroscopic properties. Continued efforts are devoted to developing biobased autonomous self-healing elastomers that combine fast and efficient healing with high mechanical strength.

#### Antimicrobial polymers and nanostructures

So far, we have described bioinspired and biomimetic materials in terms of bulk properties, but they also have unique features on the molecular level. As a case study, we in particular consider AMPs and their mimics to highlight the importance of composition and polymer chemistry on the individual macromolecular level. AMPs are short-chain cationic peptides that participate in the innate immune response of all living things<sup>173–175</sup>. AMPs have a broad spectrum of activity against bacteria, fungi, viruses and other parasites<sup>176</sup>. They provide the first line of defence against invading pathogens by direct and rapid antimicrobial action and have several roles, including immune regulation<sup>177</sup>. For example, the human cathelicidin peptide LL-37, isolated from neutrophils, is one of the most studied AMPs<sup>178,179</sup> (FIG. 6a). Cationic AMPs strongly interact with and destabilize anionic lipid bilayer membranes by forming transmembrane channels, which eventually

leads to cell death (FIG. 6b). Other modes of antimicrobial action are also observed. AMPs can exhibit secondary structures such as  $\alpha$ -helix,  $\beta$ -sheet, extended and looped structures. Helix-forming AMPs adopt the particular secondary structures only on binding anionic cell membranes, where positive charges and lipophilic groups align along opposite sides, making AMPs globally amphiphilic<sup>180</sup>. This is one of the prominent features that synthetic mimics of AMPs are designed to recapitulate (FIG. 6c). Unlike specific receptor-mediated interactions, the putative mode of AMP action relies on a few essential parameters, such as conformation, hydrophobicity and positive charge, to form amphiphilic structures and enforce non-specific interactions with cell membranes<sup>181</sup>. This aspect of AMPs and their mimics is advantageous relative to conventional antibiotics with specific high-affinity targets because microorganisms more quickly build resistance to the latter targeted modes of action. These features of natural AMPs have inspired the design of next-generation antimicrobial biomaterials that could solve the challenges posed by multidrug-resistant microorganisms. We now highlight recent developments in the *de novo* design of synthetic AMPs and AMP-inspired polymers.

**Antimicrobial peptide architectures.** The widespread use of AMPs has been hindered by their short half-lives *in vivo*, non-specific toxicity, low bioavailability and high manufacturing costs<sup>177,182,183</sup>. Two fundamental approaches have been used to improve AMP performance by altering structural features influencing antimicrobial activity and stability, including amino acid sequence, amphipathicity, hydrophobic moieties, net charge, conformation and length<sup>175,183</sup>. The first approach is a quantitative structure–activity relationship investigation that begins with a natural AMP blueprint and redesigns it by altering the sequence or shortening it<sup>184,185</sup>. The second approach is *de novo* design of synthetic peptides that is realized using computational methods to generate AMP sequences without a model sequence. Recently, computer-aided design strategies such as *de novo* drug design and machine learning have increasingly influenced AMP discovery research<sup>186</sup>. These approaches have advanced the design of synthetic AMP mimics in terms of sequence optimization, structural diversity, *in vivo* activity and improved therapeutic indices. In addition to AMP design by bioinformatic analyses of known AMP sequences or empirical design approaches, the atomic-level structural and dynamic information obtained from molecular dynamics simulations of spontaneous peptide assembly in membranes has been used to develop *de novo*, potent small pore-forming AMPs<sup>187</sup>.

The antimicrobial activity of bioinspired synthetic AMPs and related structures can be enhanced by designing ‘advanced’ molecular architectures. For example, a cationic star-like architecture has more appropriate local charge density, surface electrostatic potential and proteolytic stability<sup>188</sup>. Bioinspired structurally nano-engineered AMP polymers (SNAPPs) were conceived by random ring-opening copolymerization of cyclic *N*-carboxyanhydride derivatives of lysine and valine

starting from a dendritic poly(amidoamine) core<sup>189</sup> (FIG. 6d,e). The star-shaped peptide polymers, which bear 16 or 32 arms, formed unimolecular architectures that are stable at infinite dilution. SNAPPs exhibited submicromolar activity against Gram-negative bacteria, including colistin-resistant pathogens and *Enterococcus faecium*, *Staphylococcus aureus*, *Klebsiella pneumoniae*, *Acinetobacter baumannii*, *Pseudomonas aeruginosa* and *Enterobacter* spp., while exhibiting low toxicity. In addition, SNAPPs exerted multimodal antibacterial

activity by destabilizing the outer membrane, such that ion movement across the cytoplasmic membrane is no longer regulated and apoptotic-like death ensues. Providing higher local concentrations of SNAPPs enabled profound antimicrobial responses and lowered the risk of resistance development. A de novo peptide topology of artificial virus-like capsids was obtained by assembling de novo AMPs<sup>190</sup>. These artificial capsids, assembled as 20-nm hollow shells, rapidly attack bacterial membranes. They land on phospholipid bilayers

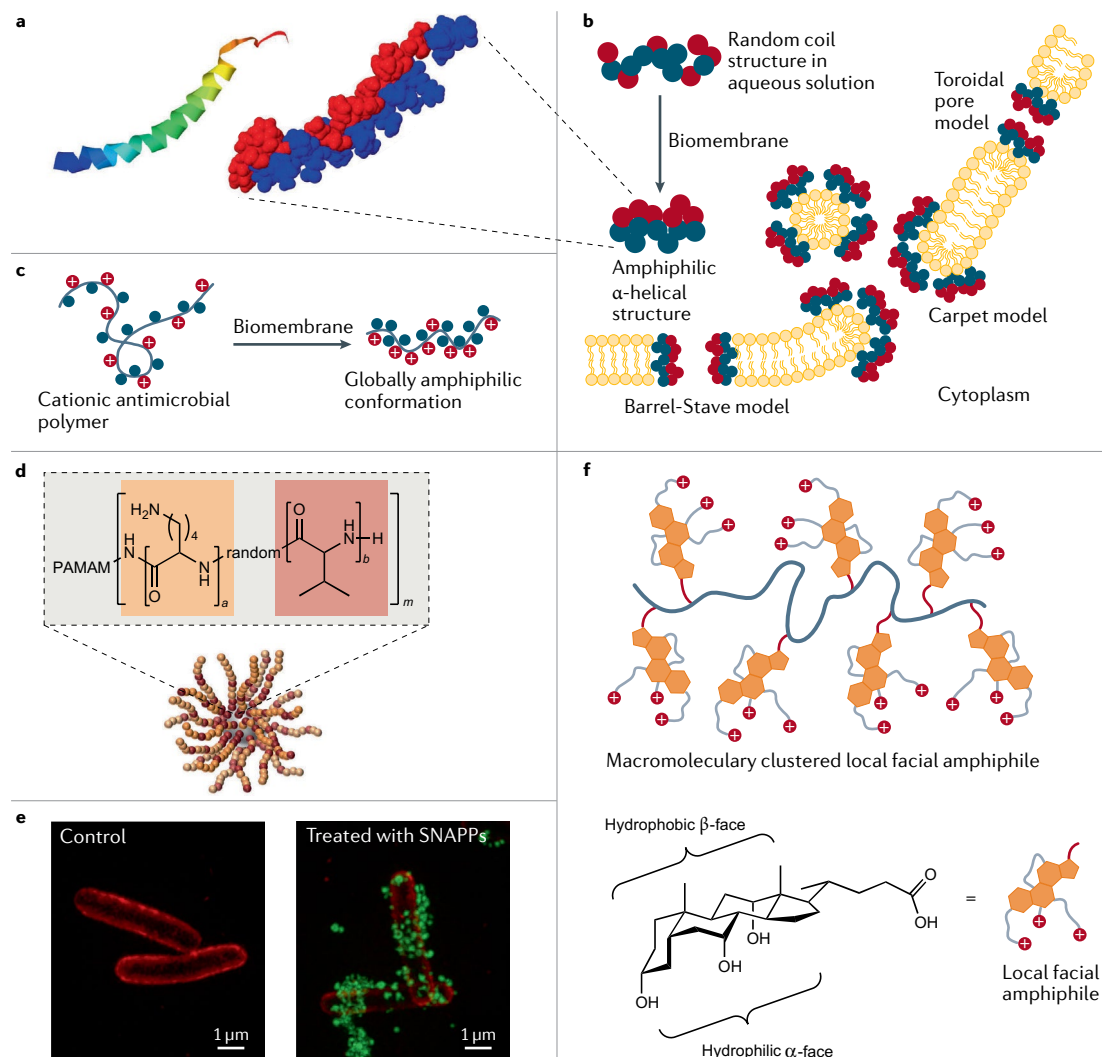


**Fig. 6 | Bioinspired and biomimetic polymers for antimicrobial applications.** **a** The antimicrobial peptide (AMP) LL-37 structure features an  $\alpha$ -helical ribbon and hydrophobic (blue) and hydrophilic (red) regions<sup>178,179</sup>. **b** AMP mechanisms of membrane disruption<sup>173,229</sup> can be modeled in different ways. In the barrel-stave and toroidal pore models, AMPs insert themselves into membranes perpendicularly, where they generate membrane-spanning aqueous channels. The AMPs contact the phospholipid head groups in the toroidal pore model. In contrast, in the carpet model, the membrane surface becomes coated with destabilizing AMPs. At higher concentrations, carpet model peptides can behave as detergents. **c** When antimicrobial polymers approach a biomembrane surface, they adopt a globally amphiphilic irregular conformation<sup>180</sup>. **d** Structurally nanoengineered antimicrobial peptide polymers (SNAPPs)<sup>189</sup> can take the form of 16- and 32-arm star peptide polymer nanoparticles with dendritic poly(amidoamine) (PAMAM) cores. **e** Optical 3D structured illumination microscopy images of *Escherichia coli* before and after treatment with AF488-tagged SNAPPs (green) with 16 arms<sup>189</sup>. The *E. coli* cell membrane was stained with FM4-64FX (red). Membrane-associated or internalized SNAPPs are visible. **f** Facially amphiphilic antimicrobial polymer mimics derived from bile acids<sup>222</sup>. These cationic antimicrobial polymers possess local facial amphiphilicity at the repeating unit level due to the presence of facially amphiphilic cationic bile acid structures. Part **a** is reprinted from REFS<sup>178,179</sup>, CC BY 4.0. Parts **d** and **e** reprinted from REF<sup>189</sup>, Springer Nature Limited. Part **f** reprinted from REF<sup>222</sup>, Springer Nature Limited.

and instantaneously induce the formation of quickly expanding pores, causing bacterial lysis within minutes. AMPs must be stabilized against protease-induced degradation, especially for in vitro applications. The stability can be increased by several methods, including the use of D-amino acids<sup>191</sup> and crosslinking<sup>192,193</sup>. The non-specific toxicity of AMPs is thought to arise from their amphipathic helical structures, hydrophobic groups and charge density. The de novo design of smart peptides, which modulate bioactivity by undergoing a random coil to helix transition, may minimize toxicity with regard to mammalian cells while maintaining high antimicrobial activity. For example, the use of phosphatase-cleavable phosphate-bearing distorted amphiphilic polypeptides proved less toxic to mammalian cells<sup>194</sup>. However, bacterial phosphatase restored the helical structure at the infection site, thus contributing to the strong membrane-disruptive antimicrobial capability.

**Bioinspired antimicrobial polymers.** Synthetic polymers have been explored as novel antimicrobial agents to prevent and treat infections<sup>195–197</sup>. Among these polymers, species containing cationic groups have been widely designed and evaluated for antimicrobial applications based on principles learned from AMPs<sup>198–200</sup>. Synthetic cationic polymers can have activity by adopting amphiphilic structures on contacting bacterial membranes. Various monomers and polymer architectures have been explored to optimize activity<sup>195</sup>. Thus, advances in controlled polymerization readily afford different polymeric architectures, such as homopolymers, random copolymers, BCPs, telechelic polymers (species with end groups that can engage in polymerization and/or other reactivity) and branched polymers. These are available for optimizing antimicrobial properties, while maintaining sufficient biocompatibility<sup>195</sup>. Antimicrobial polymers with AMP-inspired designs are based on the adoption of a globally amphiphilic conformation without the need for a specific folding pattern, as seen in AMPs (FIG. 6c). This is achieved by designing random copolymers with flexible backbones using hydrophobic and hydrophilic monomers that do not require the control of subunit sequences<sup>201</sup>. However, the preparation of sequence-controlled antimicrobial polymers by photoinduced electron transfer–reversible addition–fragmentation chain transfer polymerization demonstrated that antibacterial genus specificity could be tuned simply by changing the order of the polymer blocks along with combined modulation of polymer chain length<sup>202</sup>.

Unlike small-molecule antibiotics, properties of polymers such as hydrophilicity, molecular weight and the type/amount of positive charge can be tuned to achieve the highest antimicrobial activity and selectivity. Most antimicrobial polymers contain cationic moieties — typically ammonium<sup>203</sup>, guanidinium<sup>204,205</sup>, phosphonium<sup>206</sup>, sulfonium<sup>207</sup> and metal ions can also be present<sup>208–210</sup>. Guanidinium-containing polymers exhibited membrane translocation properties and precipitation of cytoplasmic materials<sup>211</sup>. Interestingly, some cationic antimicrobial metallopolymers showed synergistic effects with conventional antibiotics<sup>208–210</sup>. Attachment of uncharged polar moieties is an attractive method to increase the

hydrophilicity and biocompatibility of antimicrobial polymers.

Copolymerization can increase biocompatibility in conjunction with hydrophilic monomers such as hydroxyethyl methacrylate<sup>208</sup>, poly(ethylene glycol) methyl ether methacrylate<sup>212</sup> or monomers with pendant carbohydrates<sup>213</sup> and zwitterionic moieties. Antimicrobial polymers combine the synergies of natural antimicrobial small molecules with the benefits of polymeric structures, which substantially increase the local concentration of active sites. However, high molecular weight polymers may have undesirable properties such as low solubility and a propensity to undergo aggregation or the inability to diffuse through bacterial cell walls. AMP-inspired polymers with pronounced antimicrobial efficacy have molecular weights generally in the range from 2,000 to 30,000. A ‘sieving effect’ has been observed for high molecular weight polymers against Gram-positive bacteria due to the cell wall structure<sup>214</sup>. Additionally, the double-membrane structure of Gram-negative bacteria prevents antimicrobial polymers from reaching the inner membrane at sufficient concentrations.

The lessons from AMP research have contributed to progress in making biobased antimicrobial polymers. Various biopolymers have been chemically modified to yield antimicrobial polymers and composites, including polysaccharides (for example, chitosan, cellulose and starch), proteins (for example, caseinates, keratin and collagen) and biobased polymers (such as poly(lactic acid), poly(hydroxyalkanoate), poly(butylene succinate) and polyurethanes)<sup>215</sup>. Chitosan is prominent in antimicrobial polymer research because of its activity but also advantages of being non-toxic, biodegradable and biocompatible<sup>216</sup>. Cationic peptidopolysaccharides, obtained by grafting AMPs to chitosan with click chemistry, have particularly good antimicrobial activities<sup>217,218</sup>. Natural resin acids such as abietic acid and its isomers are widely abundant diterpene organic acids with fused cyclic hydrophobic structures. These resin acids are obtained from coniferous trees and have diverse applications after chemical modifications<sup>219</sup>, not least against Gram-positive bacteria such as methicillin-resistant *Staphylococcus aureus*. Importantly, they simultaneously exhibit low cytotoxicity in vitro and in vivo<sup>220,221</sup>, making them very selective.

The energetically unfavourable global amphiphilicity of cationic polymers can be circumvented by designing repeating units with local facial amphiphilicity. These structures promote interactions between the entire macromolecule and bacterial cell membranes. Antimicrobial polymers with local facial amphiphilicity were recently conceptualized using multicyclic natural bile acids, including cholic acid, deoxycholic and lithocholic acid<sup>222,223</sup> (FIG. 6f). The hydrophobic multicyclic structure and three oriented cationic charges in a cholic acid derivative provided true facial amphiphilic structures that exhibited high antimicrobial activity and selectivity (more than 98, the ratio between the concentration leading to 50% haemolysis of red blood cells and the minimum inhibitory concentration for bacterial growth) against Gram-negative bacteria. Additionally,

amphiphilic polymeric nanoparticles have been investigated as effective antimicrobial agents<sup>224</sup>. For example, environmentally benign biodegradable and biobased lignin-core nanoparticles loaded with Ag<sup>+</sup> ions and coated with cationic polyelectrolytes were developed as effective antibacterial agents<sup>225</sup>. The cationic charges of polyelectrolytes can enhance interactions with bacterial surfaces, while locally abundant Ag<sup>+</sup> ions effectively kill pathogens with minimal cytotoxicity. These examples highlight the potential for honing biobased building blocks to make effective antimicrobial agents.

In summary, biomimetic AMPs and bioinspired cationic polymers offer new avenues to tackle multidrug-resistant microorganisms, which has important medicinal implications given the increasing problem of resistance. Synthetic oligopeptides and polypeptides and advanced nanoarchitectures with smart properties have greater antimicrobial activity and stability, as well as lower toxicity. AMP bioinspiration has led to synthetic polymers with an array of complex architectures with globally amphiphilic and facially amphiphilic structural features that increase antimicrobial effectiveness. Biobased monomers and polymers have spawned great interest, and the knowledge gained in these molecular-level antimicrobial systems can be incorporated into bulk materials such as antimicrobial coatings and composites.

### Conclusions and outlook

This Review has highlighted recent progress in bioinspired and biomimetic polymer research, which has afforded materials with outstanding mechanical, adaptive, self-healing and antimicrobial properties. Materials with each of these properties have been detailed herein, but we note that most of the macroscopic properties of these materials can be traced to molecular compositions and interactions on the nanoscale and mesoscale. Creative chemical approaches are vital for successful material design through bioinspiration and biomimicry. Summarizing the chemistry of these materials at a high level is challenging. Overall, it is our view that crosslinking/networking, dynamic interactions and self-assembly (or phase separation) could be used to guide the design of

bioinspired and biomimetic materials. Mimics of resilin and spider silk, as well as mechanically adaptive composites, need to be crosslinked to produce well-defined networks. In contrast, self-healing materials, such as elastomers and hydrogels, also need crosslinking to maintain desirable mechanical properties for achieving healing. Dynamic interactions are best represented by self-healing materials, although such interactions are also present in bioactive polymers that aim to disrupt cell membranes. Self-assembly is almost universal in bioinspired materials, particularly optically adaptive polymers. The process can give combinations of crystalline domains and amorphous matrices, rigid and viscoelastic co-existing phases or hydrophobic and hydrophilic faces, all with very distinct properties.

The evolution of chemical approaches itself is dynamic, and there has been a strong emphasis on sustainability. Thus, a natural extension of bioinspired and biomimetic materials is to use biobased feedstocks, which have seen explosive growth over the last two decades. The development of sustainable polymers from renewable natural products or biomass is undergoing transformative changes as consumer demand increases. Although some bioinspired and biomimetic materials have been prepared from biobased resources, most are still based on petrochemical precursors. As this field keeps evolving, it should be emphasized that natural polymers or biobased compounds do not necessarily result in materials that are more sustainable than materials based entirely on synthetic polymers. The overall sustainability of a material can be assessed only by life-cycle analysis or similar methods that take into consideration the energy required and environmental impact to source the raw materials, the production process and the material's behaviour during and at the end of use. However, at present, using a biobased component in the preparation of bioinspired and biomimetic materials is a giant leap towards sustainable value-added applications. We hope that the concepts presented in this Review will be beneficial to advance biomimetic and bioinspired polymer chemistry along with emerging biobased compositions.

Published online 5 October 2021

- Wang, Y., Naleway, S. E. & Wang, B. Biological and bioinspired materials: structure leading to functional and mechanical performance. *Bioact. Mater.* **5**, 745–757 (2020).
- Sanchez, C., Arribart, H. & Guille, M. M. G. Biomimicry and bioinspiration as tools for the design of innovative materials and systems. *Nat. Mater.* **4**, 277–288 (2005).
- Levin, A. et al. Biomimetic peptide self-assembly for functional materials. *Nat. Rev. Chem.* **4**, 615–634 (2020).
- Montero de Espinosa, L., Meesorn, W., Moatsou, D. & Weder, C. Bioinspired polymer systems with stimulus-responsive mechanical properties. *Chem. Rev.* **117**, 12851–12892 (2017).
- Lefèvre, T. & Auger, M. Spider silk as a blueprint for greener materials: a review. *Int. Mater. Rev.* **61**, 127–153 (2016).
- Tao, H., Kaplan, D. L. & Omenetto, F. G. Silk materials — a road to sustainable high technology. *Adv. Mater.* **24**, 2824–2837 (2012).
- Muižnieks, L. D. & Keeley, F. W. Biomechanical design of elastic protein biomaterials: a balance of protein structure and conformational disorder. *ACS Biomater. Sci. Eng.* **3**, 661–679 (2017).
- Balu, R., Dutta, N. K., Dutta, A. K. & Choudhury, N. R. Resilin-mimetics as a smart biomaterial platform for biomedical applications. *Nat. Commun.* **12**, 149 (2021).
- Capadona, J. R., Shanmuganathan, K., Tyler, D. J., Rowan, S. J. & Weder, C. Stimuli-responsive polymer nanocomposites inspired by the sea cucumber dermis. *Science* **319**, 1370 (2008).
- Fratzl, P. & Weinkamer, R. Nature's hierarchical materials. *Prog. Mater Sci.* **52**, 1263–1334 (2007).
- Whitesides, G. M. Bioinspiration: something for everyone. *Interface Focus* **5**, 20150031 (2015).
- Bhushan, B. Biomimetics: lessons from nature — an overview. *Philos. Trans. A Math. Phys. Eng. Sci.* **367**, 1445–1486 (2009).
- Fratzl, P., Dunlop, J. & Weinkamer, R. *Materials Design Inspired by Nature: Function Through Inner Architecture* (Royal Society of Chemistry, 2015).
- Chee, E. & Brown, A. C. Biomimetic antimicrobial material strategies for combating antibiotic resistant bacteria. *Biomater. Sci.* **8**, 1089–1100 (2020).
- Si, Y., Dong, Z. & Jiang, L. Bioinspired designs of superhydrophobic and superhydrophilic materials. *ACS Cent. Sci.* **4**, 1102–1112 (2018).
- Nishimoto, S. & Bhushan, B. Bioinspired self-cleaning surfaces with superhydrophobicity, superoleophobicity, and superhydrophilicity. *RSC Adv.* **3**, 671–690 (2013).
- Zhu, Y., Yang, F. & Guo, Z. Bioinspired surfaces with special micro-structures and wettability for drag reduction: which surface design will be a better choice? *Nanoscale* **13**, 3463–3482 (2021).
- Chen, Y. et al. Bioinspired multiscale wet adhesive surfaces: structures and controlled adhesion. *Adv. Funct. Mater.* **30**, 1905287 (2020).
- Huang, W. et al. Multiscale toughening mechanisms in biological materials and bioinspired designs. *Adv. Mater.* **31**, 1901561 (2019).
- Shang, L., Zhang, W., Xu, K. & Zhao, Y. Bio-inspired intelligent structural color materials. *Mater. Horiz.* **6**, 945–958 (2019).
- Tao, P. et al. Bioinspired engineering of thermal materials. *Adv. Mater.* **27**, 428–463 (2015).
- Cremaldi, J. C. & Bhushan, B. Bioinspired self-healing materials: lessons from nature. *Beilstein J. Nanotechnol* **9**, 907–935 (2018).
- Wang, S. & Urban, M. W. Self-healing polymers. *Nat. Rev. Mater.* **5**, 562–583 (2020).

24. Pedersen Zari, M. Biomimetic materials for addressing climate change. in *Handbook of Ecomaterials* (eds Torres Martinez, L. M., Vasilieva Kharissova, O. & Kharisov, B. I.) 3169–3191 (Springer Nature Limited, 2019).

25. Wagh, P. & Escobar, I. C. Biomimetic and bioinspired membranes for water purification: a critical review and future directions. *Environ. Prog. Sustain. Energy* **38**, e13215 (2019).

26. Yang, G., Chen, S. & Zhang, J. Bioinspired and biomimetic nanotherapies for the treatment of infectious diseases. *Front. Pharmacol.* **10**, 751 (2019).

27. Green, J. J. & Elisseeff, J. H. Mimicking biological functionality with polymers for biomedical applications. *Nature* **540**, 386–394 (2016).

28. Lepora, N. F., Verschure, P. & Prescott, T. J. The state of the art in biomimetics. *Bioinspir. Biomim.* **8**, 013001 (2013).

29. Speck, O., Speck, D., Horn, R., Gantner, J. & Sedlbauer, K. P. Biomimetic bio-inspired biomorph sustainable? An attempt to classify and clarify biology-derived technical developments. *Bioinspir. Biomim.* **12**, 011004 (2017).

30. Wanick, K. & Beismann, H. Perception and role of standards in the world of biomimetics. *Bioinspired Biomim. Nanobiomaterials* **10**, 8–15 (2021).

31. Zhu, Y., Romain, C. & Williams, C. K. Sustainable polymers from renewable resources. *Nature* **540**, 354–362 (2016).

32. Schneiderman, D. K. & Hillmyer, M. A. 50th anniversary perspective: there is a great future in sustainable polymers. *Macromolecules* **50**, 3733–3749 (2017).

33. Wang, Z., Ganewatta, M. S. & Tang, C. Sustainable polymers from biomass: bridging chemistry with materials and processing. *Prog. Polym. Sci.* **101**, 101197 (2020).

34. Zheng, J. & Suh, S. Strategies to reduce the global carbon footprint of plastics. *Nat. Clim. Change* **9**, 374–378 (2019).

35. Hong, M. & Chen, E. Y. X. Future directions for sustainable polymers. *Trends Chem.* **1**, 148–151 (2019).

36. Heinrich, L. A. Future opportunities for bio-based adhesives — advantages beyond renewability. *Green Chem.* **21**, 1866–1888 (2019).

37. Yao, K. & Tang, C. Controlled polymerization of next-generation renewable monomers and beyond. *Macromolecules* **46**, 1689–1712 (2013).

38. Wilbon, P. A., Chu, F. & Tang, C. Progress in renewable polymers from natural terpenes, terpenoids, and rosin. *Macromol. Rapid Commun.* **34**, 8–37 (2013).

39. Fratzl, P. Biomimetic materials research: what can we really learn from nature's structural materials? *J. R. Soc. Interface* **4**, 637–642 (2007).

40. Wegst, U. G. K., Bai, H., Saiz, E., Tomsia, A. P. & Ritchie, R. O. Bioinspired structural materials. *Nat. Mater.* **14**, 23–36 (2015).

41. Wang, J., Cheng, Q., Lin, L. & Jiang, L. Synergistic toughening of bioinspired poly(vinyl alcohol)-clay-nanofibrillar cellulose artificial nacre. *ACS Nano* **8**, 2739–2745 (2014).

42. Guan, Q.-F., Yang, H.-B., Han, Z.-M., Ling, Z.-C. & Yu, S.-H. An all-natural bioinspired structural material for plastic replacement. *Nat. Commun.* **11**, 5401 (2020).

43. Kushner, A. M., Vossler, J. D., Williams, G. A. & Guan, Z. A biomimetic modular polymer with tough and adaptive properties. *J. Am. Chem. Soc.* **131**, 8766 (2009).

44. Zhang, Z., Cheng, L., Zhao, J., Zhang, H. & Yan, X. Muscle-mimetic synergistic covalent and supramolecular polymers: phototriggered formation leads to mechanical performance boost. *J. Am. Chem. Soc.* **143**, 902–911 (2021).

45. Qin, G., Hu, X., Cebe, P. & Kaplan, D. L. Mechanism of resilin elasticity. *Nat. Commun.* **3**, 1003 (2012).

46. Aeschbach, R., Amado, R. & Neukom, H. Formation of tyrosine cross-links in proteins by oxidation of tyrosine residues. *Biochim. Biophys. Acta* **439**, 292–301 (1976).

47. Du, N., Yang, Z., Liu, X. Y., Li, Y. & Xu, H. Y. Structural origin of the strain-hardening of spider silk. *Adv. Funct. Mater.* **21**, 772–778 (2011).

48. Heim, M., Keerl, D. & Scheibel, T. Spider silk: from soluble protein to extraordinary fiber. *Angew. Chem. Int. Ed.* **48**, 3584–3596 (2009).

49. Haas, F., Gorb, S. & Blickhan, R. The function of resilin in beetle wings. *Proc. R. Soc. B* **267**, 1575–1581 (2000).

50. Su, R. S.-C., Kim, Y. & Liu, J. C. Resilin: protein-based elastomeric biomaterials. *Acta Biomater.* **10**, 1601–1611 (2014).

51. Balu, R., Whittaker, J., Dutta, N. K., Elvin, C. M. & Choudhury, N. R. Multi-responsive biomaterials and nanobiocomjugates from resilin-like protein polymers. *J. Mater. Chem. B* **2**, 5936–5947 (2014).

52. Tamburro, A. M. et al. Molecular and supramolecular structural studies on significant repetitive sequences of resilin. *ChemBioChem* **11**, 83–93 (2010).

53. Partlow, B. P., Applegate, M. B., Omenetto, F. G. & Kaplan, D. L. Dityrosine cross-linking in designing biomaterials. *ACS Biomater. Sci. Eng.* **2**, 2108–2121 (2016).

54. Fancy, D. A. & Kodadek, T. Chemistry for the analysis of protein–protein interactions: rapid and efficient cross-linking triggered by long wavelength light. *Proc. Natl. Acad. Sci. USA* **96**, 6020–6024 (1999).

55. Elvin, C. M. et al. Synthesis and properties of crosslinked recombinant pro-resilin. *Nature* **437**, 999–1002 (2005).

56. Qin, G. et al. Recombinant exon-encoded resilins for elastomeric biomaterials. *Biomaterials* **32**, 9251–9243 (2011).

57. Li, L., Teller, S., Clifton, R. J., Jia, X. & Kiick, K. L. Tunable mechanical stability and deformation response of a resilin-based elastomer. *Biomacromolecules* **12**, 2302–2310 (2011).

58. McGann, C. L., Akins, R. E. & Kiick, K. L. Resilin–PEG hybrid hydrogels yield degradable elastomeric scaffolds with heterogeneous microstructure. *Biomacromolecules* **17**, 128–140 (2016).

59. Desai, M. S. et al. Elastin-based rubber-like hydrogels. *Biomacromolecules* **17**, 2409–2416 (2016).

60. Cui, J. et al. Synthetically simple, highly resilient hydrogels. *Biomacromolecules* **13**, 584–588 (2012).

61. Xiao, L., Liu, C., Zhu, J., Pochan, D. J. & Jia, X. Hybrid elastomeric hydrogels crosslinked by multifunctional block copolymer micelles. *Soft Matter* **6**, 5293–5297 (2010).

62. Tan, M., Zhao, T., Huang, H. & Guo, M. Highly stretchable and resilient hydrogels from the copolymerization of acrylamide and a polymerizable macromolecular surfactant. *Polym. Chem.* **4**, 5570–5576 (2013).

63. Zhao, T. et al. Reactive macromolecular micelle crosslinked highly elastic hydrogel with water-triggered shape-memory behaviour. *Polym. Chem.* **5**, 4965–4973 (2014).

64. Si, L. et al. Silicone-based tough hydrogels with high resilience, fast self-recovery, and self-healing properties. *Chem. Commun.* **52**, 8365–8368 (2016).

65. Zhu, M. et al. A novel highly resilient nanocomposite hydrogel with low hysteresis and ultrahigh elongation. *Macromol. Rapid Commun.* **27**, 1023–1028 (2006).

66. Nah, C., Ryu, H. J., Wan, D. K. & Chang, Y. W. Preparation and properties of acrylonitrile–butadiene copolymer hybrid nanocomposites with organoclays. *Polym. Int.* **52**, 1359–1364 (2003).

67. Wang, Z. et al. Bioinspired high resilient elastomers to mimic resilin. *ACS Macro Lett.* **5**, 220–223 (2016).

68. Yuan, L. et al. A biomass approach to mendable bio-elastomers. *Soft Matter* **13**, 1306–1313 (2017).

69. Yarger, J., Cherry, B. & van der Vaart, A. Uncovering the structure–function relationship in spider silk. *Nat. Rev. Mater.* **3**, 18008 (2018).

70. Jenkins, J., Creager, M., Butler, E., Lewis, R. & Holland, G. Solid-state NMR evidence for elastin-like beta-turn structure in spider dragline silk. *Chem. Commun.* **46**, 6714–6716 (2010).

71. Krishnaji, S. T. et al. Sequence–structure–property relationships of recombinant spider silk proteins: integration of biopolymer design, processing, and modeling. *Adv. Funct. Mater.* **23**, 241–253 (2013).

72. Venkatesan, H. et al. Artificial spider silk is smart like natural one: having humidity-sensitive shape memory with superior recovery stress. *Mater. Chem. Front.* **3**, 2472–2482 (2019).

73. An, B. et al. Reproducing natural spider silks' copolymer behavior in synthetic silk mimics. *Biomacromolecules* **13**, 3938–3948 (2012).

74. Rising, A. & Johansson, J. Toward spinning artificial spider silk. *Nat. Chem. Biol.* **11**, 309–315 (2015).

75. Leigh, T. & Fernandez-Trillo, P. Helical polymers for biological and medical applications. *Nat. Rev. Chem.* **4**, 291–310 (2020).

76. Rathore, O. & Sogah, D. Y. Self-assembly of beta-sheets into nanostructures by poly(alanine) segments incorporated in multiblock copolymers inspired by spider silk. *J. Am. Chem. Soc.* **123**, 5231–5239 (2001).

77. Yao, J. et al. Synthesis and solid-state secondary structure investigation of silk-proteinlike multiblock polymers. *Macromolecules* **36**, 7508–7512 (2003).

78. Zhou, C. et al. Synthesis and characterization of multiblock copolymers based on spider dragline silk proteins. *Biomacromolecules* **7**, 2415–2419 (2006).

79. Tsuchiya, K. & Numata, K. Chemical synthesis of multiblock copolyptides inspired by spider dragline silk proteins. *ACS Macro Lett.* **6**, 103–106 (2017).

80. Gu, L., Jiang, Y. & Hu, J. Scalable spider-silk-like supertough fibers using a pseudoprotein polymer. *Adv. Mater.* **31**, 1904311 (2019).

81. Chan, N. J. et al. Spider-silk inspired polymeric networks by harnessing the mechanical potential of beta-sheets through network guided assembly. *Nat. Commun.* **11**, 1630 (2020).

82. Wu, Y. et al. Bioinspired supramolecular fibers drawn from a multiphase self-assembled hydrogel. *Proc. Natl. Acad. Sci. USA* **114**, 8163–8168 (2017).

83. Wu, Y. et al. Biomimetic supramolecular fibers exhibit water-induced supercontraction. *Adv. Mater.* **30**, e1707169 (2018).

84. Dou, Y. et al. Artificial spider silk from ion-doped and twisted core-sheath hydrogel fibres. *Nat. Commun.* **10**, 5293 (2019).

85. Song, P. et al. Bioinspired design of strong, tough, and thermally stable polymeric materials via nanoconfinement. *ACS Nano* **12**, 9266–9278 (2018).

86. Yu, Y. et al. Biomimetic mineralized organic–inorganic hybrid macrofiber with spider silk-like supertoughness. *Adv. Funct. Mater.* **30**, 1908556 (2019).

87. Zhang, X., Liu, W., Yang, D. & Qiu, X. Biomimetic supertough and strong biodegradable polymeric materials with improved thermal properties and excellent UV-blocking performance. *Adv. Funct. Mater.* **29**, 1806912 (2019).

88. Niu, W. et al. Remalleable, healable, and highly sustainable supramolecular polymeric materials combining superhigh strength and ultrahigh toughness. *ACS Appl. Mater. Interfaces* **12**, 30805–30814 (2020).

89. Liu, L., Yang, X., Yu, H., Ma, C. & Yao, J. Biomimicking the structure of silk fibers via cellulose nanocrystal as  $\beta$ -sheet crystallite. *RSC Adv.* **4**, 14304–14313 (2014).

90. Stuart, M. A. C. et al. Emerging applications of stimuli-responsive polymer materials. *Nat. Mater.* **9**, 101–113 (2010).

91. Liu, F. & Urban, M. W. Recent advances and challenges in designing stimuli-responsive polymers. *Prog. Polym. Sci.* **35**, 3–23 (2010).

92. Theato, P., Sumerlin, B. S., O'Reilly, R. K. & Epps, T. H. III Stimuli responsive materials. *Chem. Soc. Rev.* **42**, 7055–7056 (2013).

93. Wei, M., Gao, Y., Li, X. & Serpe, M. J. Stimuli-responsive polymers and their applications. *Polym. Chem.* **8**, 127–143 (2017).

94. Gao, S. et al. Stimuli-responsive bio-based polymeric systems and their applications. *J. Mater. Chem. B* **7**, 709–729 (2019).

95. Dash, M., Chiellini, F., Ottenbrite, R. M. & Chiellini, E. Chitosan-A versatile semi-synthetic polymer in biomedical applications. *Prog. Polym. Sci.* **36**, 981–1014 (2011).

96. Nasser, R., Deutschman, C. P., Han, L., Pope, M. A. & Tam, K. C. Cellulose nanocrystals in smart and stimuli-responsive materials: a review. *Mater. Today Adv.* **5**, 100055 (2020).

97. Ionov, L. Biomimetic hydrogel-based actuating systems. *Adv. Funct. Mater.* **23**, 4555–4570 (2013).

98. Oliver, K., Seddon, A. & Trask, R. S. Morphing in nature and beyond: a review of natural and synthetic shape-changing materials and mechanisms. *J. Mater. Sci.* **51**, 10663–10689 (2016).

99. Erb, R. M., Sander, J. S., Grisch, R. & Studart, A. R. Self-shaping composites with programmable bioinspired microstructures. *Nat. Commun.* **4**, 1712 (2013).

100. Studart, A. R. & Erb, R. M. Bioinspired materials that self-shape through programmed microstructures. *Soft Matter* **10**, 1284–1294 (2014).

101. Mo, J. et al. Interfibrillar stiffening of echinoderm mutable collagenous tissue demonstrated at the nanoscale. *Proc. Natl. Acad. Sci. USA* **113**, E6362–E6371 (2016).

102. Wilkie, I. C. Mutable collagenous tissue: overview and biotechnological perspective. in *Echinodermata* (ed. Matranga, V.) 221–250 (Springer, 2005).

103. Habibi, Y., Lucia, L. A. & Rojas, O. J. Cellulose nanocrystals: chemistry, self-assembly, and applications. *Chem. Rev.* **110**, 3479–3500 (2010).

104. Jorfi, M., Roberts, M. N., Foster, E. J. & Weder, C. Physiologically responsive, mechanically adaptive bio-nanocomposites for biomedical applications. *ACS Appl. Mater. Interfaces* **5**, 1517–1526 (2013).

105. Way, A. E., Hsu, L., Shanmuganathan, K., Weder, C. & Rowan, S. J. pH-responsive cellulose nanocrystal gels and nanocomposites. *ACS Macro Lett.* **1**, 1001–1006 (2012).

106. Zhou, S. et al. Cellulose hydrogels by reversible ion-exchange as flexible pressure sensors. *Adv. Mater. Technol.* **5**, 2000358 (2020).

107. Dagnon, K. L., Shanmuganathan, K., Weder, C. & Rowan, S. J. Water-triggered modulus changes of cellulose nanofiber nanocomposites with hydrophobic polymer matrices. *Macromolecules* **45**, 4707–4715 (2012).

108. Song, L., Wang, Z., Lamm, M. E., Yuan, L. & Tang, C. Supramolecular polymer nanocomposites derived from plant oils and cellulose nanocrystals. *Macromolecules* **50**, 7475–7483 (2017).

109. Wang, B. et al. Cellulose nanocrystal/plant oil polymer composites with hydrophobicity, humidity-sensitivity, and high wet strength. *Carbohydr. Polym.* **231**, 115739 (2020).

110. Kai, D. et al. Towards lignin-based functional materials in a sustainable world. *Green Chem.* **18**, 1175–1200 (2016).

111. Ganewatta, M. S., Lokupitiya, H. N. & Tang, C. Lignin biopolymers in the age of controlled polymerization. *Polymers* **11**, 1176 (2019).

112. Moreno, A. & Sipponen, M. H. Lignin-based smart materials: a roadmap to processing and synthesis for current and future applications. *Mater. Horiz.* **7**, 2237–2257 (2020).

113. Dallmeyer, I., Chowdhury, S. & Kadla, J. F. Preparation and characterization of kraft lignin-based moisture-responsive films with reversible shape-change capability. *Biomacromolecules* **14**, 2354–2363 (2013).

114. Dai, L. et al. All-lignin-based hydrogel with fast pH-stimuli responsiveness for mechanical switching and actuation. *Chem. Mater.* **32**, 4324–4330 (2020).

115. Cuthill, I. C. et al. The biology of color. *Science* **357**, eaan0221 (2017).

116. Tadepalli, S., Slocik, J. M., Gupta, M. K., Naik, R. R. & Singamneni, S. Bio-optics and bio-inspired optical materials. *Chem. Rev.* **117**, 12705–12763 (2017).

117. Shawkey, M. D. & D'Alba, L. Interactions between colour-producing mechanisms and their effects on the integumentary colour palette. *Philos. Trans. R. Soc. B* **372**, 20160536 (2017).

118. Isapour, G. & Lattuada, M. Bioinspired stimuli-responsive color-changing systems. *Adv. Mater.* **30**, 1707069 (2018).

119. Teysier, J., Saenko, S. V., van der Marel, D. & Milinkovich, M. C. Photonic crystals cause active colour change in chameleons. *Nat. Commun.* **6**, 6368 (2015).

120. van Heeswijk, E. P. A., Kragt, A. J. J., Grossiord, N. & Schenning, A. P. H. J. Environmentally responsive photonic polymers. *Chem. Commun.* **55**, 2880–2891 (2019).

121. Xiong, R. et al. Biopolymeric photonic structures: design, fabrication, and emerging applications. *Chem. Soc. Rev.* **49**, 983–1031 (2020).

122. Kose, O., Tran, A., Lewis, L., Hamad, W. Y. & MacLachlan, M. J. Unwinding a spiral of cellulose nanocrystals for stimuli-responsive stretchable optics. *Nat. Commun.* **10**, 510 (2019).

123. Fernandes, S. N. et al. Mind the microgap in iridescent cellulose nanocrystal films. *Adv. Mater.* **29**, 1603560 (2017).

124. Yao, K., Meng, Q., Bulone, V. & Zhou, Q. Flexible and responsive chiral nematic cellulose nanocrystal/poly(ethylene glycol) composite films with uniform and tunable structural color. *Adv. Mater.* **29**, 1701323 (2017).

125. Giese, M. & Spengler, M. Cellulose nanocrystals in nanoarchitectonics – towards photonic functional materials. *Mol. Sys. Des. Eng.* **4**, 29–48 (2019).

126. Xu, M. et al. Multifunctional chiral nematic cellulose nanocrystals/glycerol structural colored nanocomposites for intelligent responsive films, photonic inks and iridescent coatings. *J. Mater. Chem. C* **6**, 5391–5400 (2018).

127. Zhang, Z.-L. et al. Chameleon-inspired variable coloration enabled by a highly flexible photonic cellulose film. *ACS Appl. Mater. Interfaces* **12**, 46710–46718 (2020).

128. Boott, C. E., Tran, A., Hamad, W. Y. & MacLachlan, M. J. Cellulose nanocrystal elastomers with reversible visible color. *Angew. Chem. Int. Ed.* **59**, 226–231 (2020).

129. Armstrong, E. & O'Dwyer, C. Artificial opal photonic crystals and inverse opal structures – fundamentals and applications from optics to energy storage. *J. Mater. Chem. C* **3**, 6109–6143 (2015).

130. Wang, Y., Li, M. & Wang, Y. Silk: a versatile biomaterial for advanced optics and photonics. *Chin. Opt. Lett.* **18**, 080004 (2020).

131. Wang, Y. et al. Design, fabrication, and function of silk-based nanomaterials. *Adv. Funct. Mater.* **28**, 1805305 (2018).

132. Kim, S. et al. Silk inverse opals. *Nat. Photon.* **6**, 818–823 (2012).

133. Wang, Y. et al. Modulation of multiscale 3D lattices through conformational control: painting silk inverse opals with water and light. *Adv. Mater.* **29**, 1702769 (2017).

134. Swinerd, V. M., Collins, A. M., Skaer, N. J. V., Gheysens, T. & Mann, S. Silk inverse opals from template-directed  $\beta$ -sheet transformation of regenerated silk fibroin. *Soft Matter* **3**, 1377–1380 (2007).

135. Wang, Y., Li, M., Colusso, E., Li, W. & Omenetto, F. G. Designing the iridescences of biopolymers by assembly of photonic crystal superlattices. *Adv. Opt. Mater.* **6**, 1800066 (2018).

136. Appold, M., Grune, E., Frey, H. & Gallei, M. One-step anionic copolymerization enables formation of linear ultrahigh-molecular-weight block copolymer films featuring vivid structural colors in the bulk state. *ACS Appl. Mater. Interfaces* **10**, 18202–18212 (2018).

137. Appold, M. & Gallei, M. Bio-inspired structural colors based on linear ultrahigh molecular weight block copolymers. *ACS Appl. Polym. Mater.* **1**, 239–250 (2019).

138. Urbas, A. et al. Tunable block copolymer/homopolymer photonic crystals. *Adv. Mater.* **12**, 812–814 (2000).

139. Liberman-Martin, A. L., Chu, C. K. & Grubbs, R. H. Application of bottlebrush block copolymers as photonic crystals. *Macromol. Rapid Commun.* **38**, 1700058 (2017).

140. Miyake, G. M., Weitekamp, R. A., Piunova, V. A. & Grubbs, R. H. Synthesis of isocyanate-based brush block copolymers and their rapid self-assembly to infrared-reflecting photonic crystals. *J. Am. Chem. Soc.* **134**, 14249–14254 (2012).

141. Xia, Y., Olsen, B. D., Kornfield, J. A. & Grubbs, R. H. Efficient synthesis of narrowly dispersed brush copolymers and study of their assemblies: the importance of side chain arrangement. *J. Am. Chem. Soc.* **131**, 18525–18532 (2009).

142. Sveinbjörnsson, B. R. et al. Rapid self-assembly of brush block copolymers to photonic crystals. *Proc. Natl. Acad. Sci. USA* **109**, 14332 (2012).

143. Patel, B. B. et al. Tunable structural color of bottlebrush block copolymers through direct-write 3D printing from solution. *Sci. Adv.* **6**, eaaz7202 (2020).

144. Yang, Y., Ding, X. & Urban, M. W. Chemical and physical aspects of self-healing materials. *Prog. Polym. Sci.* **49**, 34–59 (2015).

145. Feng, Z. et al. Photothermal-induced self-healable and reconfigurable shape memory bio-based elastomer with recyclable ability. *ACS Appl. Mater. Interfaces* **11**, 1469–1479 (2019).

146. Lamm, M. E. et al. Tuning mechanical properties of biobased polymers by supramolecular chain entanglement. *Macromolecules* **52**, 8967–8975 (2019).

147. Lu, C. et al. Sustainable multiple- and multistimulus-shape-memory and self-healing elastomers with semi-interpenetrating network derived from biomass via bulk radical polymerization. *ACS Sustain. Chem. Eng.* **6**, 6527–6535 (2018).

148. Zeng, C., Seino, H., Ren, J., Hatanaka, K. & Yoshie, N. Bio-based furan polymers with self-healing ability. *Macromolecules* **46**, 1794–1802 (2013).

149. Amaral, A. J. R. & Pasparakis, G. Stimuli responsive self-healing polymers: gels, elastomers and membranes. *Polym. Chem.* **8**, 6464–6484 (2017).

150. Kim, S. M. et al. Superior toughness and fast self-healing at room temperature engineered by transparent elastomers. *Adv. Mater.* **30**, 1705145 (2018).

151. Lee, S., Shin, S. & Lee, D. Self-healing of cross-linked PU via dual-dynamic covalent bonds of a Schiff base from cysteine and vanillin. *Mater. Des.* **172**, 107774 (2019).

152. Cromwell, O., Chung, J. & Guan, Z. Malleable and self-healing covalent polymer networks through tunable dynamic boronic ester bonds. *J. Am. Chem. Soc.* **137**, 6492–6495 (2015).

153. Wang, P., Deng, G. H., Zhou, L. Y., Li, Z. Y. & Chen, Y. M. Ultrastretchable, self-healable hydrogels based on dynamic covalent bonding and triblock copolymer micellization. *ACS Macro Lett.* **6**, 881–886 (2017).

154. Tanasi, P., Santana, M. H., Carretero-Gonzalez, J., Verdejo, R. & Lopez-Manchado, M. A. Thermo-reversible crosslinked natural rubber: a Diels–Alder route for reuse and self-healing properties in elastomers. *Polymer* **175**, 15–24 (2019).

155. Feng, Z. et al. Environmentally friendly method to prepare thermo-reversible, self-healable biobased elastomers by one-step melt processing. *ACS Appl. Polym. Mater.* **1**, 169–177 (2019).

156. Shao, C., Wang, M., Chang, H., Xu, F. & Yang, J. A self-healing cellulose nanocrystal–poly(ethylene glycol) nanocomposite hydrogel via Diels–Alder click reaction. *ACS Sustain. Chem. Eng.* **5**, 6167–6174 (2017).

157. Hernández, M. et al. Turning vulcanized natural rubber into a self-healing polymer: effect of the disulfide/polysulfide ratio. *ACS Sustain. Chem. Eng.* **4**, 5776–5784 (2016).

158. Cordiner, P., Tournilhac, F., Soulie-Ziakovic, C. & Leibler, L. Self-healing and thermoreversible rubber from supramolecular assembly. *Nature* **451**, 977–980 (2008).

159. Chuanhui, X., Nie, J., Wu, W., Zheng, Z. & Chen, Y. Self-healable, recyclable, and strengthened epoxidized natural rubber/carboxymethyl chitosan biobased composites with hydrogen bonding supramolecular hybrid networks. *ACS Sustain. Chem. Eng.* **7**, 15778–15789 (2019).

160. Nakahata, M., Takashima, Y., Yamaguchi, H. & Harada, A. Redox-responsive self-healing materials formed from host–guest polymers. *Nat. Commun.* **2**, 511 (2011).

161. Zhang, L. et al. A highly efficient self-healing elastomer with unprecedented mechanical properties. *Adv. Mater.* **31**, 1901402 (2019).

162. Xu, C., Cao, L., Lin, B., Liang, X. & Chen, Y. Design of self-healing supramolecular rubbers by introducing ionic cross-links into natural rubber via a controlled vulcanization. *ACS Appl. Mater. Interfaces* **8**, 17728–17737 (2016).

163. Taylor, D. L. & Panhuis, M. I. H. Self-healing hydrogels. *Adv. Mater.* **28**, 9060–9093 (2016).

164. Wei, Z. et al. Self-healing gels based on constitutional dynamic chemistry and their potential applications. *Chem. Soc. Rev.* **43**, 8114–8131 (2014).

165. Yang, X. et al. Highly efficient self-healable and dual responsive cellulose-based hydrogels for controlled release and 3D cell culture. *Adv. Funct. Mater.* **27**, 1703174 (2017).

166. Liu, H. et al. Self-healing polysaccharide hydrogel based on dynamic covalent enamine bonds. *Macromol. Mater. Eng.* **301**, 725–732 (2016).

167. Zheng, W. J., Gao, J., Wei, Z., Zhou, J. & Chen, Y. M. Facile fabrication of self-healing carboxymethyl cellulose hydrogels. *Eur. Polym. J.* **72**, 514–522 (2015).

168. Shao, C., Chang, H., Wang, M., Xu, F. & Yang, J. High-strength, tough, and self-healing nanocomposite physical hydrogels based on the synergistic effects of dynamic hydrogen bond and dual coordination bonds. *ACS Appl. Mater. Interfaces* **9**, 28305–28318 (2017).

169. Hussain, I. et al. Hydroxyethyl cellulose-based self-healing hydrogels with enhanced mechanical properties via metal–ligand bond interactions. *Eur. Polym. J.* **100**, 219–227 (2018).

170. Yang, X. et al. Scalable manufacturing of real-time self-healing strain sensors based on brominated natural rubber. *Chem. Eng. J.* **389**, 124448 (2020).

171. Cao, L., Yuan, D., Xu, C. & Chen, Y. Biobased, self-healable, high strength rubber with tunicate cellulose nanocrystals. *Nanoscale* **9**, 15696–15706 (2017).

172. Wu, M. et al. Strong autonomic self-healing biobased polyamide elastomers. *Chem. Mater.* **32**, 8325–8332 (2020).

173. Bahar, A. A. & Ren, D. Antimicrobial peptides. *Pharmaceuticals* **6**, 1543–1575 (2013).

174. Nakatsuji, T. & Gallo, R. L. Antimicrobial peptides: old molecules with new ideas. *J. Invest. Dermatol.* **132**, 887–895 (2012).

175. Fjell, C. D., Hiss, J. A., Hancock, R. E. W. & Schneider, G. Designing antimicrobial peptides: form follows function. *Nat. Rev. Drug Discov.* **11**, 37–51 (2012).

176. Janssen, H., Hamill, P. & Hancock, R. E. W. Peptide antimicrobial agents. *Clin. Microbiol. Rev.* **19**, 491–511 (2006).

177. Hancock, R. E. W. & Sahl, H.-G. Antimicrobial and host-defense peptides as new anti-infective therapeutic strategies. *Nat. Biotechnol.* **24**, 1551–1557 (2006).

178. Wang, G. Structures of human host defense cathelicidin LL-37 and its smallest antimicrobial

peptide KR-12 in lipid micelles. *J. Biol. Chem.* **283**, 32637–32643 (2008).

179. RCSB. RSCB Protein Data Bank. <http://www.rcsb.org/3d-view/jsmol/2k6o> (2020).

180. Mowery, B. P., Lindner, A. H., Weisblum, B., Stahl, S. S. & Gellman, S. H. Structure–activity relationships among random nylon-3 copolymers that mimic antibacterial host-defense peptides. *J. Am. Chem. Soc.* **131**, 9735–9745 (2009).

181. Wade, D. et al. All-D amino acid-containing channel-forming antibiotic peptides. *Proc. Natl Acad. Sci. USA* **87**, 4761 (1990).

182. Nederberg, F. et al. Biodegradable nanostructures with selective lysis of microbial membranes. *Nat. Chem.* **3**, 409–414 (2011).

183. Luong, H. X., Thanh, T. T. & Tran, T. H. Antimicrobial peptides—advances in development of therapeutic applications. *Life Sci.* **260**, 118407 (2020).

184. Torres, M. D. T., Sothiselvam, S., Lu, T. K. & de la Fuente-Nunez, C. Peptide design principles for antimicrobial applications. *J. Mol. Biol.* **431**, 3547–3567 (2019).

185. Gomes, B. et al. Designing improved active peptides for therapeutic approaches against infectious diseases. *Biotechnol. Adv.* **36**, 415–429 (2018).

186. Cardoso, M. H. et al. Computer-aided design of antimicrobial peptides: are we generating effective drug candidates? *Front. Microbiol.* **10**, 3097 (2020).

187. Chen, C. H. et al. Simulation-guided rational *de novo* design of a small pore-forming antimicrobial peptide. *J. Am. Chem. Soc.* **141**, 4839–4848 (2019).

188. Lu, C. et al. Molecular architecture and charging effects enhance the *in vitro* and *in vivo* performance of multi-arm antimicrobial agents based on star-shaped poly(l-lysine). *Adv. Therap.* **2**, 1900147 (2019).

189. Lam, S. J. et al. Combating multidrug-resistant Gram-negative bacteria with structurally nanoengineered antimicrobial peptide polymers. *Nat. Microbiol.* **1**, 16162 (2016).

190. De Santis, E. et al. Antimicrobial peptide capsids of *de novo* design. *Nat. Commun.* **8**, 2263 (2017).

191. Hong, S. Y., Oh, J. E. & Lee, K.-H. Effect of d-amino acid substitution on the stability, the secondary structure, and the activity of membrane-active peptide. *Biochem. Pharmacol.* **58**, 1775–1780 (1999).

192. Cui, H.-K. et al. Diaminodiacid-based solid-phase synthesis of peptide disulfide bond mimics. *Angew. Chem. Int. Ed.* **52**, 9558–9562 (2013).

193. Mourtada, R. et al. Design of stapled antimicrobial peptides that are stable, nontoxic and kill antibiotic-resistant bacteria in mice. *Nat. Biotechnol.* **37**, 1186–1197 (2019).

194. Xiong, M. et al. Bacteria-assisted activation of antimicrobial polypeptides by a random-coil to helix transition. *Angew. Chem. Int. Ed.* **56**, 10826–10829 (2017).

195. Ganewatta, M. S. & Tang, C. Controlling macromolecular structures towards effective antimicrobial polymers. *Polymer* **63**, A1–A29 (2015).

196. Jain, A. et al. Antimicrobial polymers. *Adv. Healthcare Mater.* **3**, 1969–1985 (2014).

197. Konai, M. M., Bhattacharjee, B., Ghosh, S. & Haldar, J. Recent progress in polymer research to tackle infections and antimicrobial resistance. *Biomacromolecules* **19**, 1888–1917 (2018).

198. Ergene, C., Yasuhara, K. & Palermo, E. F. Biomimetic antimicrobial polymers: recent advances in molecular design. *Polym. Chem.* **9**, 2407–2427 (2018).

199. Tew, G. N., Scott, R. W., Klein, M. L. & DeGrado, W. F. *De novo* design of antimicrobial polymers, foldamers, and small molecules: from discovery to practical applications. *Acc. Chem. Res.* **43**, 30–39 (2010).

200. Kuroda, K. & Caputo, G. A. Antimicrobial polymers as synthetic mimics of host-defense peptides. *WIREs Nanomed. Nanobiotechnol.* **5**, 49–66 (2013).

201. Mowery, B. P. et al. Mimicry of antimicrobial host-defense peptides by random copolymers. *J. Am. Chem. Soc.* **129**, 15474–15476 (2007).

202. Judzewitsch, P. R., Nguyen, T.-K., Shamugam, S., Wong, E. H. H. & Boyer, C. Towards sequence-controlled antimicrobial polymers: effect of polymer block order on antimicrobial activity. *Angew. Chem. Int. Ed.* **57**, 4559–4564 (2018).

203. Xue, Y., Xiao, H. & Zhang, Y. Antimicrobial polymeric materials with quaternary ammonium and phosphonium salts. *Int. J. Mol. Sci.* **16**, 3626–3655 (2015).

204. Gabriel, G. J. et al. Synthetic mimic of antimicrobial peptide with nonmembrane-disrupting antibacterial properties. *Biomacromolecules* **9**, 2980–2983 (2008).

205. Locock, K. E. S. et al. Guanylated polymethacrylates: a class of potent antimicrobial polymers with low hemolytic activity. *Biomacromolecules* **14**, 4021–4031 (2013).

206. Cuthbert, T. J. et al. Surprising antibacterial activity and selectivity of hydrophilic polyphosphoniums featuring sugar and hydroxy substituents. *Angew. Chem. Int. Ed.* **57**, 12707–12710 (2018).

207. Zhang, B., Li, M., Lin, M., Yang, X. & Sun, J. A convenient approach for antibacterial polypeptides featuring sulfonium and oligo(ethylene glycol) subunits. *Biomater. Sci.* **8**, 6969–6977 (2020).

208. Zhang, J. et al. Antimicrobial metallopolymers and their bioconjugates with conventional antibiotics against multidrug-resistant bacteria. *J. Am. Chem. Soc.* **136**, 4873–4876 (2014).

209. Zhu, T. et al. Metallo-polyelectrolytes as a class of ionic macromolecules for functional materials. *Nat. Commun.* **9**, 4329 (2018).

210. Zhu, T., Zhang, J. & Tang, C. Metallo-polyelectrolytes: correlating macromolecular architectures with properties and applications. *Trends Chem.* **2**, 227–240 (2020).

211. Chin, W. et al. A macromolecular approach to eradicate multidrug resistant bacterial infections while mitigating drug resistance onset. *Nat. Commun.* **9**, 917 (2018).

212. Sellenet, P. H., Allison, B., Applegate, B. M. & Youngblood, J. P. Synergistic activity of hydrophilic modification in antibiotic polymers. *Biomacromolecules* **8**, 19–23 (2007).

213. Colak, S., Nelson, C. F., Nüsslein, K. & Tew, G. N. Hydrophilic modifications of an amphiphilic polynorbornene and the effects on its hemolytic and antibacterial activity. *Biomacromolecules* **10**, 353–359 (2009).

214. Lienkamp, K., Kumar, K.-N., Som, A., Nüsslein, K. & Tew, G. N. “Doubly selective” antimicrobial polymers: how do they differentiate between bacteria? *Chem. Eur. J.* **15**, 11710–11714 (2009).

215. Muñoz-Bonilla, A., Echeverría, C., Sonseca, Á., Arrieta, M. P. & Fernández-García, M. Bio-based polymers with antimicrobial properties towards sustainable development. *Materials* **12**, 641 (2019).

216. Sahariah, P. & Mässon, M. Antimicrobial chitosan and chitosan derivatives: a review of the structure–activity relationship. *Biomacromolecules* **18**, 3846–3868 (2017).

217. Pranantyo, D., Xu, L. Q., Kang, E.-T. & Chan-Park, M. B. Chitosan-based peptidopolysaccharides as cationic antimicrobial agents and antibacterial coatings. *Biomacromolecules* **19**, 2156–2165 (2018).

218. Su, Y. et al. Cationic peptidopolysaccharides synthesized by ‘click’ chemistry with enhanced broad-spectrum antimicrobial activities. *Polym. Chem.* **8**, 3788–3800 (2017).

219. Kugler, S., Ossowicz, P., Malarczyk-Matusiak, K. & Wierzbicka, E. Advances in rosin-based chemicals: the latest recipes, applications and future trends. *Molecules* **24**, 1651 (2019).

220. Chen, Y. et al. Amphiphatic antibacterial agents using cationic methacrylic polymers with natural rosin as pendant group. *RSC Adv.* **2**, 10275–10282 (2012).

221. Ganewatta, M. S. et al. Bio-inspired resin acid-derived materials as anti-bacterial resistance agents with unexpected activities. *Chem. Sci.* **5**, 2011–2016 (2014).

222. Rahman, M. A. et al. Macromolecular-clustered facial amphiphilic antimicrobials. *Nat. Commun.* **9**, 5231 (2018).

223. Ganewatta, M. S. et al. Facially amphiphilic polyionene biocidal polymers derived from lithocholic acid. *Bioact. Mater.* **3**, 186–193 (2018).

224. Lam, S. J., Wong, E. H. H., Boyer, C. & Qiao, G. G. Antimicrobial polymeric nanoparticles. *Prog. Polym. Sci.* **76**, 40–64 (2018).

225. Richter, A. P. et al. An environmentally benign antimicrobial nanoparticle based on a silver-infused lignin core. *Nat. Nanotechnol.* **10**, 817–823 (2015).

226. Nova, A., Keten, S., Pugno, N. M., Redaelli, A. & Buehler, M. J. Molecular and nanostructural mechanisms of deformation, strength and toughness of spider silk fibrils. *Nano Lett.* **10**, 2626–2634 (2010).

227. de Jong, E., Higson, A., Walsh, P. & Wellisch, M. Product developments in the bio-based chemicals arena. *Biofuels Bioprod. Bioref.* **6**, 606–624 (2012).

228. Kim, Y., Gill, E. E. & Liu, J. C. Enzymatic crosslinking of resilin-based proteins for vascular tissue engineering applications. *Biomacromolecules* **17**, 2530–2539 (2016).

229. Wimley, W. C. Describing the mechanism of antimicrobial peptide action with the interfacial activity model. *ACS Chem. Biol.* **5**, 905–917 (2010).

#### Acknowledgements

This project has received partial funding from the US National Science Foundation (DMR-1806792 to C.T.) and the US National Institutes of Health (R01AI149810 to C.T.). Z.W. thanks Anhui Agricultural University for support.

#### Author contributions

M.S.G. and Z.W. contributed equally to this work. M.S.G., Z.W. and C.T. conceived the Review. All authors contributed to the discussion and writing of the Review.

#### Competing interests

The authors declare no competing interests.

#### Publisher's note

Springer Nature remains neutral with regard to jurisdictional claims in published maps and institutional affiliations.

© Springer Nature Limited 2021